

DRAFT

ALTRO and TPC Performance of ALICE

Roland Bramm
Dissertation 2005

DRAFT

Content

ALICE	1	Computing	39
TPC	1	Pedestals	39
ALTRO	1	TCF	39
Roland Bramm	1	BSC2 & ZSU	40
Dissertation 2004	1	Configuration	40
The Experiment	1	Literaturverzeichniss	43
The Experiment	2	The Experiment	44
TPC	2	Front End Electronic	45
Requirements	3	Jitter	45
Working principle	3	Prototype Environment	45
Gas Ionisation	4	ALTRO Parameter Optimising	46
Electron/Ion Drift	5	Pulse Finder	48
Electron Diffusion	5	Pedestal Calculation log	48
Readout Chamber	6	make coefficients	49
Signal creation	7	Correlator	50
Prototype	7		
Front End Electronic	11		
The Front End Electronic	12		
FEC	12		
PASA	12		
ALTRO	13		
ADC	13		
BCSI	13		
TCF	14		
BSC2	14		
ZSU	15		
DFU	15		
MEB	15		
Backplane	16		
RCU	16		
SIU	16		
DCS	16		
Jitter	19		
Jitter	20		
Simulation	20		
Result	21		
Prototype Environment	25		
Prototype	26		
IROC & Mapping	26		
Data Aquisition and Configuration	26		
Data Format One	27		
Data Format Two	27		
Monitoring	27		
Test Beam	28		
Configuration	28		
Readout	29		
Data Storage	29		
Data Format	29		
Monitoring	30		
HLT	31		
ALTRO Parameter Optimising	33		
Parameter Optimising	34		
BCS1 Parameters	34		
Extraction	34		
Result	34		
Baseline Dispersion	35		
TCF Parameters	35		
Pulse Finder	35		
Parameter Set Finder	36		
Correlator	36		
Best Set Finder	36		
BSC2 & ZSU Parameters	38		
Altro++	39		

The Experiment

The Experiment

ALICE (**A** Large Ion Collider Experiment)[1-5] is an experiment at the LHC (**L**arge **H**adron Collider) with the goal to study heavy ion collisions up to the top energy available. It is designed to study the physics of strongly interacting matter and the QGP (**Q**uark **G**luon **P**lasma). The experimental setup is shown in the picture below.

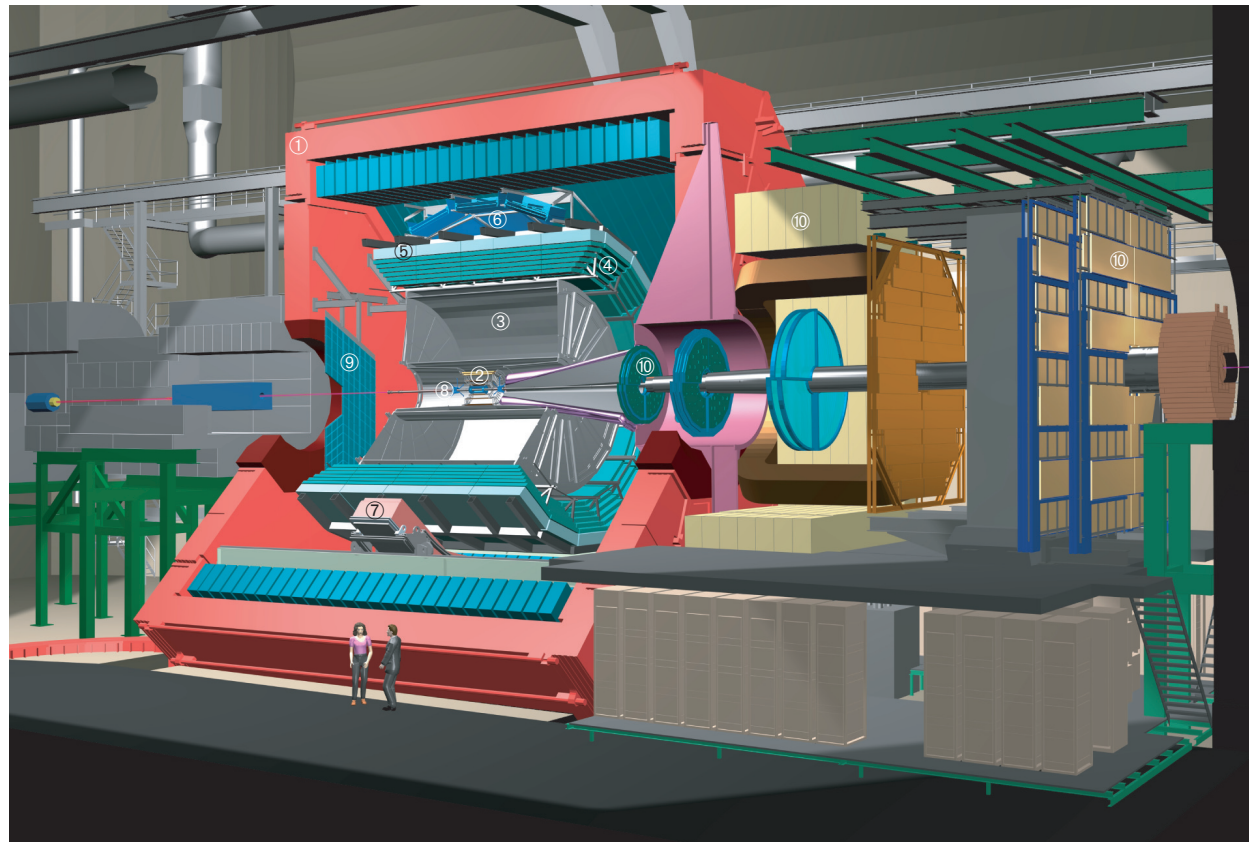
In general the detectors are highly capable to measure and identify hadrons, leptons and photons around mid rapidity over a broad range from very low (100 MeV) up to fairly high (100 GeV) impulses. In addition there is a myon arm ⑩ [6] which covers the detection at large rapidities ($-4 < \eta < -2.4$). In a moderate magnetic field of up to 0.5 T provided by the reused and modernised L3 Magnet ① [32] are positioned the central detectors which are covering the mid rapidity region ($-0.9 < \eta < 0.9$). A big part of ALICE also covers 360° in ϕ in this region. For tracking the main detectors the ITS (Inner Tracking System, ②) [7] as a silicon based detector, the TPC (Time Projection Chamber, ③) [8] and a highly granular TRD (Transition Radiation Detector, ④) [9] are used, this set is called central barrel. For particle identification the TPC measurement of the energy loss (dE/dx), the transition radiation of the TRD and the time of flight of the TOF (Time Of Flight, ⑤) [10] is used. In addition there is the HMPID (High Momentum Particle Identification Detector, ⑥) [11] for high momentum particles, and a photon spectrometer PHOS (Photon Spectrometer, ⑦) [12] for photon measurements, these two detectors do not have the full 360° acceptance in ϕ . There

are fast detectors for the trigger at large rapidities like the FMD (Forward Multiplicity Detector, ⑧) [13], V0 and T0 at ($-3.4 < \eta < -5.1$) [14,15] for measuring charged particles and a narrower band for photons ($2.3 < \eta < 3.5$) with the PMD (Photon Multiplicity Detector, ⑨) [16]. At last there are two ZDC (Zero Degree Calorimeters) [17], to measure the spectator nucleons at beam rapidity.

TPC

A time projection chamber (TPC) provides a complete, 3D picture of the ionization deposited in a gas volume. It acts similar like a bubble chamber, however with a fast and purely electronic readout. This 3D “imagine” capability defines the usefulness as a tracking device in a high track density environment and for the identification of particles through their ionisation energy loss (dE/dx). Therefore it is the main tracking detector in the central barrel of the ALICE experiment. The usage as a large acceptance tracking and identification detector in heavy ion experiments starts with NA49 [18] and STAR (Solenoidal Tracker At RHIC) [19] at the SPS (Super Proton Synchrotron) and RHIC (Relativistic Heavy Ion Collider), respectively.

A TPC consists of mainly three parts, the drift chamber, the readout chamber and the front end electronics. The field cage surrounds the detector gas and provides a homogenous electrical field to transport the electrons of the ionisation to the readout chamber. This is also the sensitive volume of a TPC. The readout chamber amplifies the signal and provides the coupling to the gas for the front end electronics. Here the signal is again amplified, shaped,



The ALICE experiment

digitised, processed, stored and then send to the data acquisition.

Requirements

The physics program foreseen determines the exigencies at the ALICE TPC alone and in conjunction with other detectors. The hadron physics demands:

- » **Two TRACK RESOLUTION:** The two track resolution has to be sufficient to allow a HBT [??] measurement with a resolution in relative momentum of a few (< 5) MeV.
- » **dE/dx RESOLUTION:** The dE/dx resolution should be at least 8% or better to properly identify hadrons.
- » **TRACK MATCHING:** For fast decaying particles a proper (85% - 95%) matching capability of the TPC to ITS or TOF or both is needed.

For leptonic observables the demands are partially different:

- » **TRACKING EFFICIENCY:** Since electron pairs are most interesting, a tracking efficiency of at least 90% for tracks at $p_t > 1\text{GeV}/c$ should be achieved.
- » **MOMENTUM RESOLUTION:** To get a good mass resolution (< 100 MeV) for heavy mesons like the Υ , the momentum resolution for electrons of about 4 GeV should be at least 2.5%.
- » **dE/dx RESOLUTION:** For electrons the dE/dx resolution should be better than 10%. In cooperation with the TRD this leads to a electron to pion separation of more than a factor of 1000.
- » **RATE CAPABILITY:** For the inspection of electrons the TPC should work at 200 Hz at heavy ion collisions.

For the proton running of ALICE the demands are partly lower because of the low multiplicity but on the other hand higher since the TPC has to run at a higher rate due to the high luminosity.

- » **RATE CAPABILITY:** Due to the high luminosity in proton running the TPC has to operate at 1kHz or more to minimise the effect of pile up.

These demands lead to a design of a quite conventional TPC, but with many new resolutions in the detail. The major facets are:

- » **ACCEPTANCE:** The acceptance of the TPC matches the one of the ITS, TRD and TOF. For event by event studies as well as for all rare observables a considerable big acceptance is necessary to collect enough statistics. This leads to a size as shown in table at the end of this section.
- » **MATERIAL BUDGET:** To minimise the effect of multiple scattering and secondary particle production the material amount should be minimised. This determines the light field cage material as well as the gas choice.
- » **FIELD CAGE:** To match the rate exigencies the field cage has to provide a high field of 400 V/cm which implies a voltage greater than 100 kV at the central membrane.

» **READOUT CHAMBERS:** The readout chamber covers a area of 33 m^2 at the two endcaps of the field cage and is built as conventional multiwire proportional chamber. To fullfill the necessary accuracy in dE/dx and position resolution, as well as momentum resolution, there will be about 560000 readout pads.

» **ELECTRONICS:** As close as possible to the readout chambers the electronics for these 560000 pads have to reside, this demands a highly integrated system.

» **INTELLIGENT READOUT:** Even after the zero suppression directly in the detector electronics an event is still 60 MB in size. The data throughput when reading out at the highest detector readout rate exceeds the allowed throughput to a permanent storage by roughly a factor of 10. To get the highest acquisition rate for special events (e.g. high momentum jets, Υ particle, ...) a HLT (**High Level Trigger**) [20] is foreseen to find candidates for this events online.

Size	length	5m
	inner radius	80cm
	outer radius	250cm
Gas	composition	Ne/N2/CO2 90/5/5
	volume	88m ³
	Drift field	400 V/cm
	Drift velocity	2.85 cm/us
	Drift time	88 us
FEE	#channels	557568
	Signal/Nosie	30:1
	dynamic Range	900:1
	Noise(ENC)	1000 e
	Crosstalk	< 0.3% / -60 db
	Power Consumption	< 100mW
	max dead time	10%
Event size	Pb Pb central	85 MB
	p p	1-2 MB
Trigger rate	Pb Pb central	200 Hz
	p p	1000 Hz

Technical data of the ALICE TPC

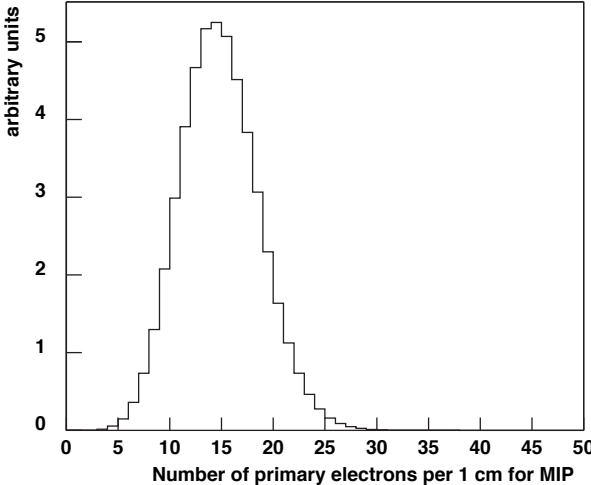
Working principle

Starting from a particle running through the gas of the drift chamber it ionises the gas molecules, so a track of ions remains along the particle trajectory. The electrical field applied from the fieldcage now lets this electron cloud drift with a constant velocity in field direction away from the central membrane towards the two readout chambers. There the signal will be amplified by avalanche creation and read out on the pad plane. Then the front end electronics electrically amplifies shapes and digitises the signal. The x and y coordinate are defined by the pad and the row coor-

dinate of the pad plane in the readout chamber. The z coordinate is defined as the drift time of the electron cloud.

Gas Ionisation

A charged particle running through a gas can ionise gas molecules, so it produces primary electrons. The statistics of the primary interactions implies a Poisson distribution of a number of primary electrons as shown below.



Distribution of numbers of primary electrons per 1 cm for a MIP in 90% Ne & 10% CO₂ [8]

The distance in between the collisions is described by an exponential [21]

$$P(l) = \frac{1}{\lambda} e^{-\frac{l}{\lambda}} \quad (f1)$$

with l as the distance between two successive collisions and λ as the mean distance between primary ionisations

$$\lambda = \frac{1}{N_{\text{prim}} \cdot f(\beta\gamma)} \quad (f2)$$

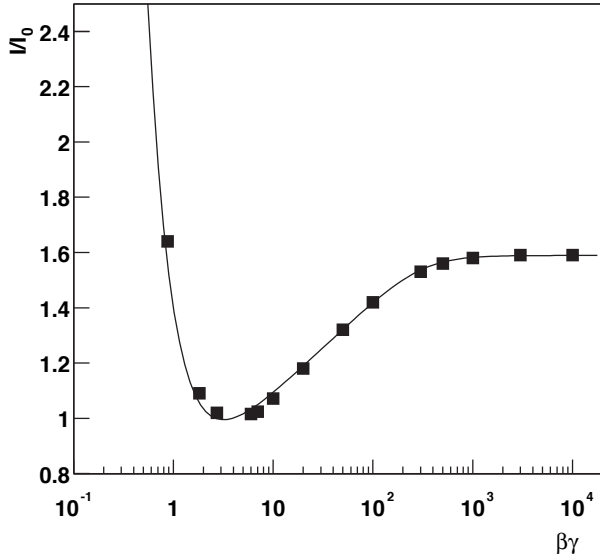
where N_{prim} is the number of primary electrons per centimeter produced by a MIP (Minimum Ionising Particle) and $f(\beta\gamma)$ as the Bethe Bloch curve [22,23].

$$\frac{dE}{dx} = \frac{4\pi Ne^4}{mc^2\beta^2} z^2 \left(\ln \frac{2mc^2\beta^2\gamma^2}{I} - \beta^2 \right) \quad (f3)$$

Based on the proposed parametrisation of the ALEPH (Apparatus for LEP Physics) [21] collaboration

$$f(\beta\gamma) = \frac{P_1}{\beta^{P_4}} \cdot \left\{ P_2 - \beta^{P_4} - \ln \left[P_3 + \frac{1}{(\beta\gamma)^{P_5}} \right] \right\} \quad (f3)$$

with the parameters $P_1=0.762 \cdot 10^{-1}$, $P_2=10.632$, $P_3=0.134 \cdot 10^{-4}$, $P_4=1.863$, $P_5=1.948$, the energy loss data for 90% Argon & 10% CH₄ [21,24] is shown in the figure below.



Bethe Bloch curve for 90% Argon and 10% CH₄, data from [21]

This is also used in the simulation due to the lack of energy loss data in the $1/\beta^2$ region and of the behaviour of Neon being quite similar to the Argon based mixtures. [24] With sufficient energy the primary electron can ionise atoms so it produces additional secondary electrons. The total number of electrons in an electron cluster is described with:

$$N_{\text{tot}} = \frac{E_{\text{tot}} - I_{\text{pot}}}{W_i} + 1 \quad (f4)$$

with E_{tot} is the energy loss in a given collision, W_i the effective energy required to produce an electron ion pair and I_{pot} is the first ionisation potential. This clusters are treated pointlike, so primary and secondary electrons are treated indifferent. This is justified because the effective range of low energy electrons is small. [8]

To optimise the signal to noise ratio, the number of produced electrons should be as high as possible, which leads to a heavier gas but also an increasing space charge due to the higher electron production and the lower ion mobility which leading to a higher occupancy.

Gas	roh[g/l]	X0[g/cm ²]	X0[m]	nmp[1/cm]
helium	0.1785	94.32	5280	2.7
neon	0.89990	28.94	322	16
argon	1.784	19.55	110	38
krypton	3.733	11.34	30.4	63
xenon	5.887	8.48	14.4	115
ref rob[26]				

Parameters of the noble gases used in TPCs

Taking the maximum multiplicity at LHC of $dn/dy \sim 6000$ [26] the heavy gases are ruled out. Finally, since the TPC is

the second innermost detector the material budget should be minimised, so this speaks in favour for a light gas.

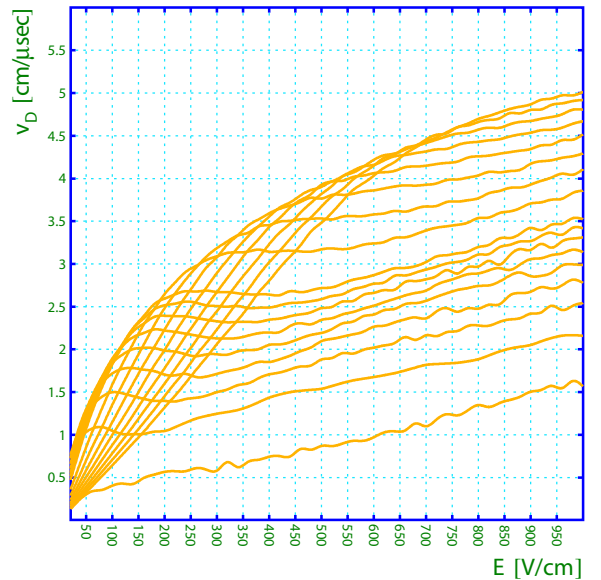
Electron/Ion Drift

In the influence of the homogeneous electrical field, as provided from the fieldcage the electron cloud moves with a constant speed towards the readout chamber. The drift speed v_d is a dynamical equilibrium of the acceleration due to the drift field and the stopping due to the collisions with the gas atoms. For the drift speed v_d is:

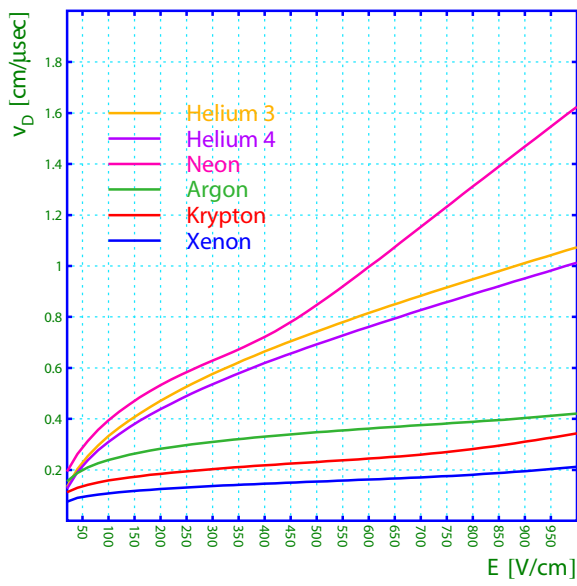
$$v_d = \frac{e}{\sqrt{2m_e}} \cdot \frac{1}{\sigma(\epsilon)\sqrt{\epsilon}} \cdot \frac{E}{N} \quad (f5)$$

with E as the electrical field and N the density of the gas. The drift speed changes with the effective cross section $\sigma(\epsilon)$ dependent on the kinetic energy of the electrons.

The drift speed as function of the field is shown in the figure below for different gases. For the high rates of the TPC the drift speed has to be quite high. For a drift time of 90 μ s the drift field has to be 400 V/cm. Warum Gas+Co2 = vd groesser ...ref in bild



When adding minimal amounts of CO₂ to neon, the drift velocity at low fields of this gased increases rapidly. The lowest curve is for the pure gas, the following for 0.25%, 0.5%, ..., 1.75%, 2%, 3%, ..., 9%, 10% [25]



Pure noble gases have low drift speed [25]

Ions drift at much lower speed (~1000 times slower than the electrons) in the opposite direction towards the central membrane. When comparing Argon and Neon the mobility of Neon is twice that of Argon. Helium has a extremely high drift speed due to its light mass, but it is difficult to be contained due to its high leak rate.

Electron Diffusion

The drift speed of one single electron differs from the mean motion of the electron cloud due to the statistical process of the scattering. These electrons follow a thermal energy distribution (Maxwell distribution) [27]:

$$F(\epsilon) = \sqrt{\frac{4\epsilon}{\pi k^3 T^3}} \cdot e^{-\frac{\epsilon}{kT}} \quad (f52)$$

The mean thermal energy is defined by the integral:

$$\langle \epsilon \rangle = \int_0^{\infty} \epsilon F(\epsilon) d\epsilon = \frac{3}{2} kT = \bar{\epsilon} \quad (f53)$$

So the electron cloud will widen up during the drift time. Starting with a point-like electron cloud at $t = 0$ and the assumption of an constant broadening the cloud will get a gaussian-shaped density distribution:

$$n = \left(\frac{1}{\sqrt{4\pi D t}} \right)^3 \cdot e^{-\frac{r^2}{4Dt}} \quad (f6)$$

with

$$r^2 = x^2 + y^2 + (z - vt)^2 \quad (f7)$$

and D as the diffusion coefficient calculated via the use of the mean free path:

$$D = \frac{1}{3} \bar{v} \lambda(\epsilon) \quad (f8)$$

The width of (f6) is

$$\sigma_x = \sqrt{2Dt} = \sqrt{\frac{2DL}{\mu E}} = \sqrt{\frac{4\epsilon L}{3eE}} \quad (f9)$$

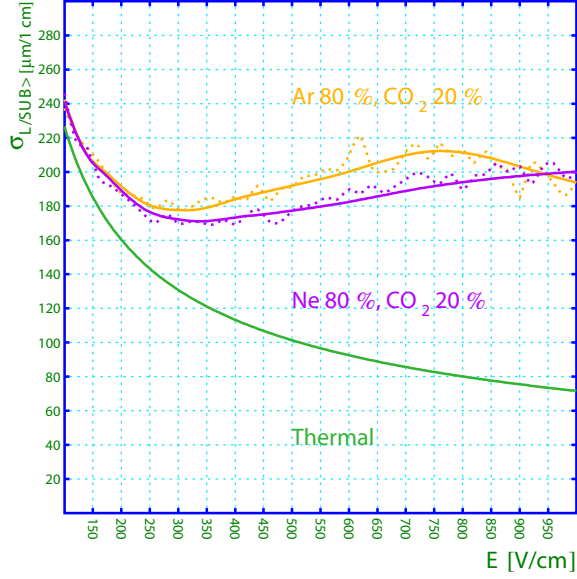
when using

$$v = \mu E \quad (f10)$$

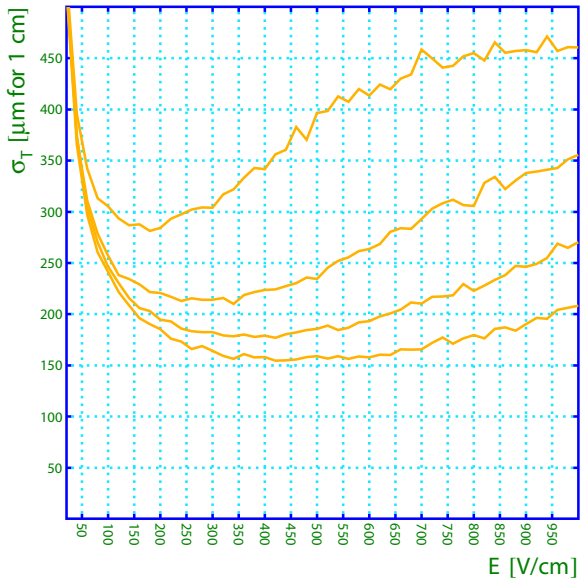
and the Nernst-Townsend formula [28]:

$$\frac{D}{\mu} = \frac{kT}{e} \quad (f11)$$

To get a small σ_x at high drift fields small electron energies are required. In Argon a field strength of 1 V/cm already produces electron energies larger than the thermal energy, so Argon is called “Hot Gas”. On the contrary, for CO_2 this behaviour occurs at fields of 2 kV/cm, so it is a “Cold Gas”. The reason is a large energy loss due to the internal degrees of freedom which are already accessible at low collision energies. In ALICE the gas mixture of Neon is foreseen. To reduce the effect of the diffusion CO_2 is added.



Longitudinal diffusion coefficient in 80% Neon 20% CO_2 approaches the thermal limit at low fields. Dashed lines are for $B = 0\text{T}$ and solid lines for $B = 0.5\text{T}$. [25]



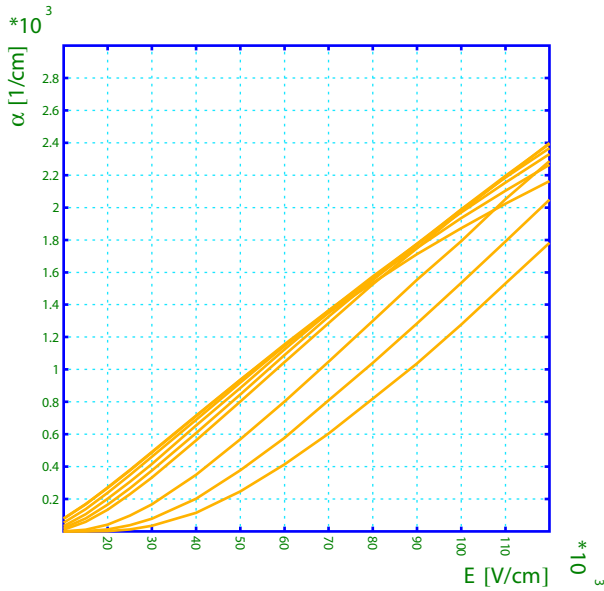
Transverse diffusion for Neon mixed with, from top to bottom, 5%, 10%, 15%, 20% CO_2 . These curves are calculated without magnetic field. [25]

Readout Chamber

The readout chamber is based on a commonly used scheme of an anode wires grid above the pad plane, a cathode wire grid and a gating grid. An electron which reaches the anode wire plane will react to the strong field induced by this plane, and will be accelerated. The energy deposited in the electron is enough to ionise the gas so at this point the opposite behaviour as in the drifting region is desired. The newly produced electron is also accelerated and ionises another gas atom so, as the number of electrons multiplies in this successive generations, the avalanche continues to grow until all electrons are collected by the anode wire. The remaining ions in between the cathode and anode plane drift towards the cathode wire grid and are mostly collected there. The processes in detail are quite complicated as there is ionisation, multiple ionisation, optical and metastable excitations and recombinations and energy transfer by collisions between atoms. The signal reaching the readout chamber is proportional to the number of produced electrons. The readout chamber in this type of TPC is also known as MWPC (Multi Wire Proportional Chamber). The multiplication of ionisation is described by the Townsend coefficient α . The increase of the number of electrons is given by:

$$dN = N\alpha ds \quad (f12)$$

Due to the several processes which are included in α no fundamental description exists and it has to be measured or simulated for every gas mixture. For the NeCO_2 mixture, α is calculated using Magboltz [29] as shown in the graph below.



The Townsend coefficient for neon mixed with, from top to bottom, 0%, 5%, 10%, 15%, 20%, 25%, 50%, 75%, 100% CO_2 .[25]

The gain in connection to the applied potential is a key feature of a proportional chamber. The gain factor M describes the ratio of the produced electrons n and the initial electrons n_0 . When using the Townsend coefficient, M can be expressed by:

$$M = \frac{n}{n_0} = \exp \left(\int_{x_0}^{x_1} \alpha(x) dx \right) \quad (f13)$$

Gas Gain Alice ... Argon vs Neon

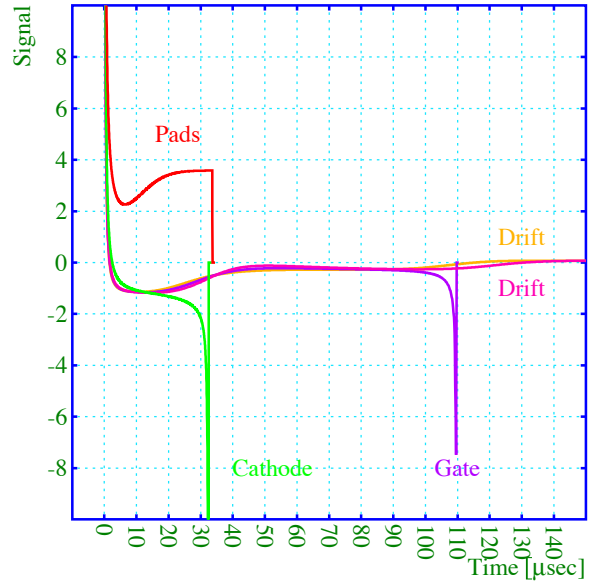
There is one effect which would spoil the space resolution when using a noble gas since during the avalanche creation also photons are produced which have a bigger cruising range and can have energies which are enough to ionise atoms. So they could create another avalanche at a different place which would result into a fake cluster not belonging to a particle track from the collision. In addition, this load when exceeding the Raether limit [30] could generate spark discharges producing aging effects or possibly destroying the readout chamber. When adding a gas with a high photoabsorption crosssection this photons are captured early and the readout chamber can be driven with a higher field and therefore with an higher amplification factor. A quencher gas is an organic gas due to the high number of degrees of freedom. In ALICE, CO_2 is used as a quencher.

Signal creation

The electrons drift towards the anode wire grid and are collected there. This induces a fast rise of a few ps of the read out signal on the pad plane. The ions are drifting much slower (~1000 times) towards the cathode plane, therefore away from the pad plane. They are inducing a mirror charge on the pad plane. The measured signal now shows a slow decay of a few μs .

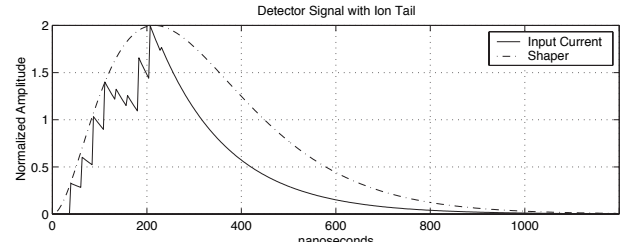
The ion velocity is higher, when they just leave the anode wire due to the smaller diameter and therefore a higher

field. This creates a positive peak. The induced signal is shown in for different ion drift targets.



Plots of collections of signals for the five different targets, showing the spread in drift time needed to reach the gate and cathode wires.

For the ions drifting towards the pad plane the signal is unipolar due to the field pointing towards the plane. The ions drifting to the cathode or gate wire grid, the product of the drift velocity and the field changes sign inducing a negative current between the avalanche wire and the cathode wire. The observed signal is bipolar and is represented in the undershoot. The amplitude of the undershoot as well as the secondary peak and the zero cross time vary with the geometry and gas of the chamber. The ions are also accelerated towards the gating grid which induces a secondary lower peak. Due to the angular spread around the anode wire and the relative strength of the fields in between the cathode wire plane and the pad plane the signal induced in the cathode wire is typically more frequent than the pad signal.



Integrated shape of several avalanche processes including the ion tail [31]

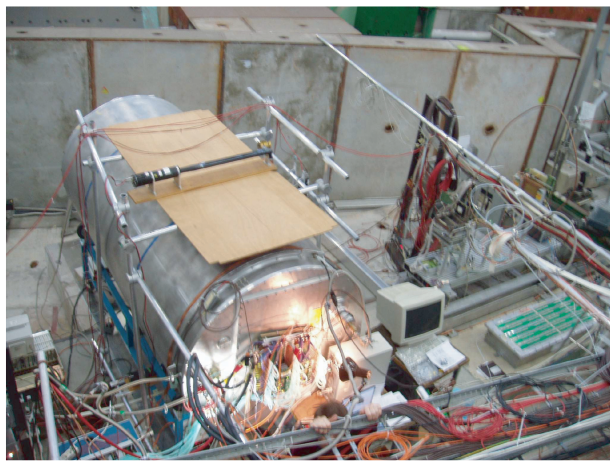
Each avalanche signal is the result of the contribution of many positive ions leaving the anode wires in various angles. An amplifier shaper integrates the signal over several avalanche processes producing a pulse with a long falling tail as shown in the plot above. The width of the pulse

depends on the track inclination, the drift length and the diffusion. [31]

The electrons are accelerated towards the anode wire grid, creating an avalanche process and are collected there. The remaining ions are drifting much slower (-1000 times) towards the cathode plane, therefore away from the pad plane. They are inducing a mirror charge on the pad plane. Some ions are collected by the pad plane or the gating grid wires. Each avalanche signal is the result of the contribution of a large number of positive ions leaving the anode wire in various angles, so following different paths which can last for several tens of microseconds inducing the long ion tail [ref neues paper]. chck ...>

Prototype

A small prototype was build to do a TPC performance test. It consists of one IROC (Inner Readout Chamber) module on one side and a complete fieldcage with a central membrane in a gas tight aluminium box. First tests were done to verify the electrostatic behaviour without a readout system. Later for the complete TPC performance test, it was equipped with four FEC boards and a triggering setup using scintillators for cosmic rays. At this time the front end cards were uncooled and the test TPC was flooded with ArCO₂. Later a simple cooling setup and four additional cards were added and the Gas was changed to NeCO₂. The cooling system is based on a underpressure liquid cooling and a copper shielding around the FEC as shown in the FEE chapter. This setup was used to gather some statistics of cosmic particles on MIPs as the most probable particle, showers as an estimate for the high multiplicity environment and particles with a big ionisation to see saturation effects, as also since two different gas mixtures were used to study differences in the signals. The data is available at [33]



Picture of the prototype setup at the PS testbeam.

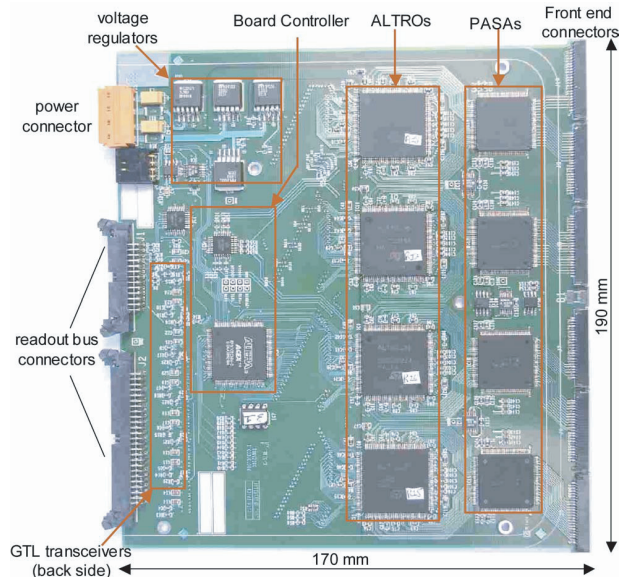
Front End Electronic

The Front End Electronic

The FEE (Front End Electronics) of the ALICE TPC has to cope with some significant design considerations. Due to the needed temperature stability in the TPC, the heat dissipation has to be minimised. The huge number of pads requires the electronics have to be highly integrated and in addition the high readout rate makes an intelligent readout mandatory. To minimise the heat dissipation, the electronics is cooled and the power consumption is minimised. The space consumption was minimised in packing several channels into each circuit and also combine analog and digital electronics in one chip as well as packing many channels on one FEC. For the high rate, the sampling speed, the processing power and the transfer bandwidth are maximised. The on detector electronics consist of the FEC and the RCU with the daughterboards DCS and SIU. The off-detector electronics consists of the DIU, RORC, DAQ and HLT.[n9]

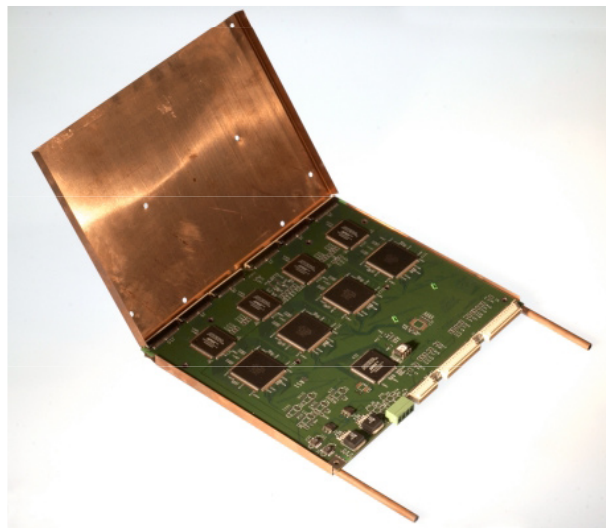
FEC

The FEC (Front End Card) contains 128 complete readout channels. The signal flow starts at the detector end with the analogue signal transported through six flexible kapton cables and the connectors. The PASA has short connexion links to this connectors, to minimise the crosstalk caused by the fast input signal from the detector. Afterwards the ALTROs are directly connected to the PASAs using differential signals. With the ALTRO the analogue part of the FEC ends and also the digital part starts. The digital outputs are multiplexed through a LVCMOS (Low Voltage CMOS) bus and translated to the GTL (Gunning Transceiver Logic) level and linked to the connectors of the backplane. In addition there is a BC (Board Controller) realised as a FPGA (Field Programmable Gate Array) which provides an independent access to the FEC via the I²C (Inter-IC) link. This is used to control the state of the voltage regulators and monitor the board activity, power supplies and temperatures, so it represents the slow control. The FEC PCB (Printed Circuit Board) contains four signal layers and four power layers divided into two supply layers and two ground layers.



Picture of the FEC PCB with all components. The Signal flows from the right through the connectors, the PASA, the ALTRO the GTL trancievers and the connectors.

In total the FEC has a maximum power consumption of 6 W. The FECs are located directly on the end caps of the TPC and with the strict temperature requirements the heat dissipation of the FEE has to be minimised. For this reason the FEC is embedded in a water cooled tray made from copper plate as shown in the picture below. [n1]



Picture of the FEC in the copper cooling plates. This plate design is to be refined since it introduces additional noise in the signal measurement

PASA

The charge collected by a TPC pad is amplified and integrated using the PASA (Preamplifier/Shaper). It has a low input impedance amplifier which is based on a CSA (Charge Sensitive Amplifier) followed by a semi Gaussian pulse shaper of the fourth order. (formula+plot) The PASA is implemented in the AMS CMOS [???] (Complementary

Metal Oxide Semiconductor) $0.35\text{ }\mu\text{m}$ technology, and consists like the ALTRO of 16 channels with a power consumption of $11\text{ mW}/\text{channel}$. The conversion gain is 12 mV/fC and the output has a dynamic range of 2 V with a differential non-linearity of 0.2 \% . The output is a pulse (picture) with a shaping time (FWHM: **Full Width Half Maximum**) of 190 ns . The noise of one single channel is below 570 electrons (RMS: **Root Mean Square**) and a channel to channel crosstalk below -60 db .[n1,n13]

ALTRO

The ALTRO (**ALICE TPC readout**) [n1,n3,n4,n5,n9] is a chip specially designed for the needs of the ALICE TPC consisting of an analog part in addition to a digital part. There are 16 channels integrated in one IC (**Integrated Circuit**), realised as $0.25\text{ }\mu\text{m}$ CMOS process operating concurrently on the analog signals coming from 16 independent inputs. Each of this channels is composed of an ADC (**Analog Digital Converter**) as the analog part, a BCSI (**Baseline Correction and Subtraction I**), a TCF (**Tail Cancellation Filter**), again a BCSII (**Baseline Correction and Subtraction II**), a ZSU (**Zero Suppression Unit**), a DFU (**Data Formatting Unit**) and a MEB (**Multi Event Buffer**), as the digital part. In addition, there is a central CCL (**Common Control Logic**) for the configuration and control for the trigger and bus. There are two frequency domains one is driven by the bus clock and consists of the Bus Interface in the CCL and the memory in the MEB and the other is driven by the readout clock and consists of the rest. Since 95% of the ALTRO runs with the sampling clock, the influence of the readout clock on the signal is minimised. The ALTRO is continuously sampling the input, on arrival of a first level trigger (L1) an event is temporarily stored in the memory. The maximum length of an event is 1008 samples. Upon arrival of a second level trigger (L2) the latest acquisition is frozen and kept until readout from the memory by the RCU via the ALTRO bus. The MEB has a capacity of eight events. Is there another

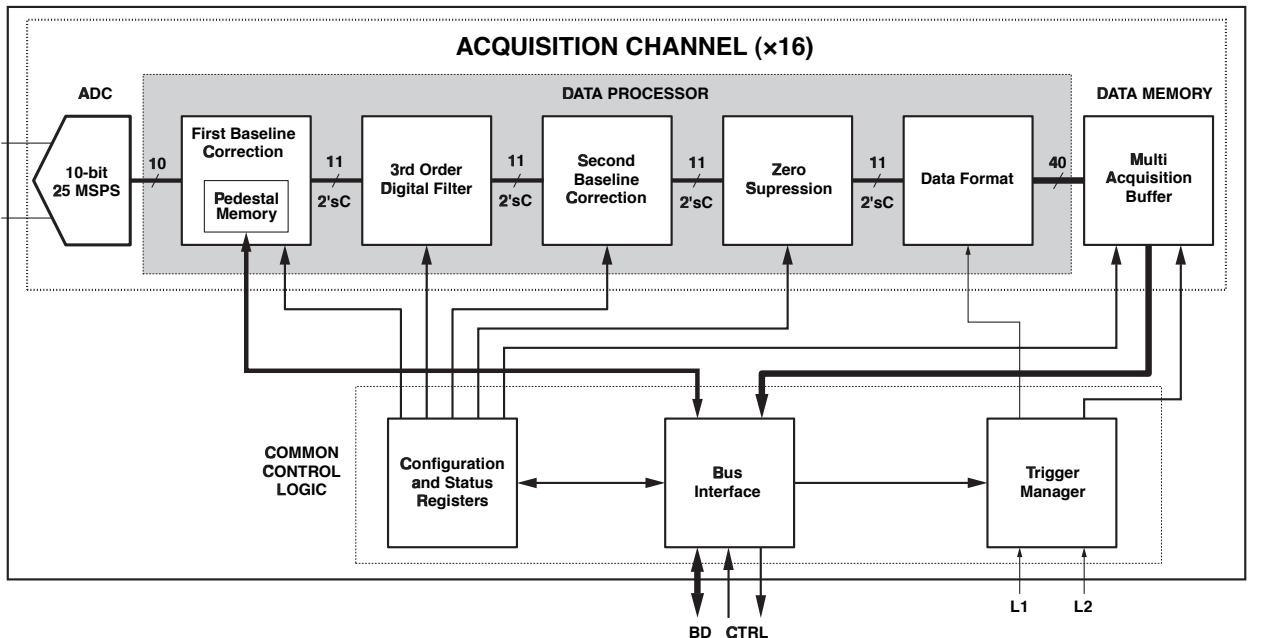
level one trigger signal prior to second level trigger the first acquisition is discarded and overwritten by the next.

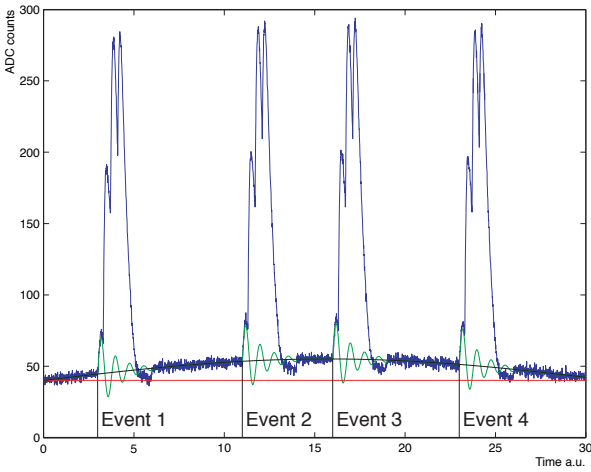
ADC

The ADC of the ALTRO is based on a commercial design, the Microelectronics TSA1001 [n2] and was slightly modified for the needs defined by ALICE. The TSA1001 was chosen because of the low power consumption which is a quite important prerequisite of the TPC, since there are extremely tight temperature constrains [n6]. The dynamic range is 10 bit and the sampling frequency is up to 25 MSPS (**Million Samples Per Second**). Due to the fact that there is a analogue part and a digital part on the ALTRO the electrical coupling has to be minimised to not decrease the quality of the sampling.

BCSI

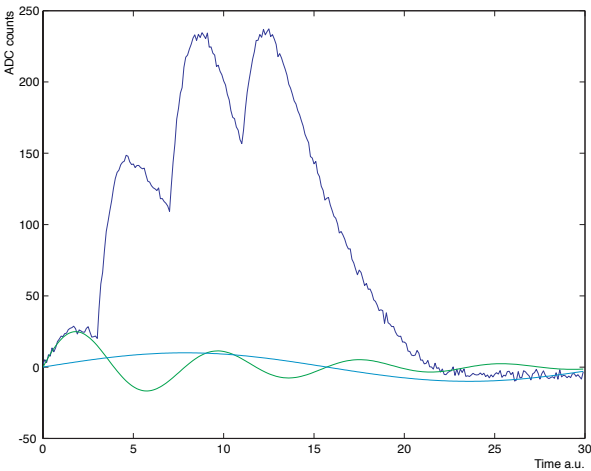
In the digital block the first unit is the baseline correction, its main purpose is the preparation of the signals for the adjacent tail cancellation unit. This unit demands the removal of the DC level and a relatively stable baseline during the data acquisition and in between. There are several sources of perturbations which can have an impact on the signal. A source of perturbations are low frequency ($<1\text{ kHz}$) variations, which are nearly constant during an acquisition window. The origin of these are temperature variations in the electronics, coupling of AC or DC and the finite detector load [n17,n18]. The self calibration circuit (AUTOCAL) of the ALTRO removes these disturbances. Since the ALTRO is continuously sampling and processing the input signal it can detect these slow variations outside the data acquisition window. This self calibration is stopped in arrival of a level one trigger and the last value is taken as DC level of the baseline which is then removed from the signal. Past a level two Trigger the calibration is re-enabled.





In this picture a low frequency perturbation as the black line is shown, the ALTRO AUTOCAL circuit detects and the BCSI removes this perturbation.

Another source of perturbations are systematic signals like the switching of the gating grid (->TPC). The removal of these is based on a LuT (Look up Table) which is realised as a memory in the ALTRO. This table is extracted from acquired empty events which means a normal data acquisition of the TPC just without tracks from a collision (->Configuration).



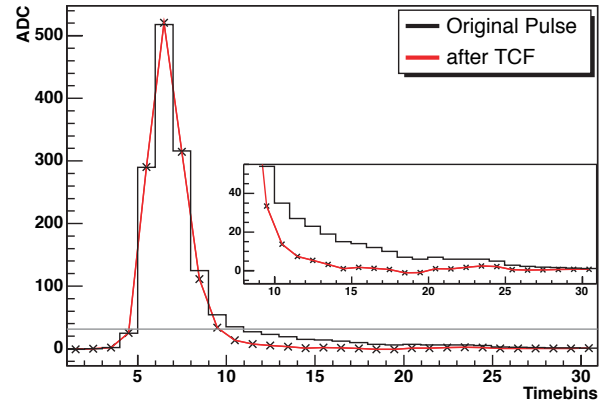
In this picture systematic perturbation the green line is shown, this is removed by the use of the LuT.

In addition the gain calibration can also be performed by this unit. The activation and the combinations of this different sub entities is configurable by several predefined set-ups as described in the ALTRO manual [n5].

TCF

The ALTRO was optimised for the TPC type used in ALICE (ref->TPC) and the presequest PASA with the semi gaussian shaping signal. This combination creates signals with a fast rise time (>1 ns) followed by a long tail. The effectiveness of the later following zero suppression is not efficient when the expected signal density is taken into ac-

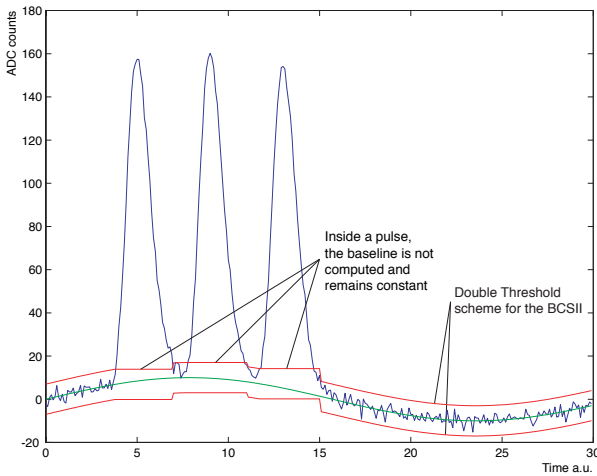
count. The problems are the long signal tail by itself in addition to the pile up effect when several signals are occurring in a short time. To improve this situation the signal tail is removed by this entity. It is implemented by a cascade of three first order IIR (Infinite Impulse Response) filter circuits and described in [n7,n8]. Each of this circuits has a set of two parameters. So in total there are six parameters to accommodate the TCF to the real signal shape. (ref->AltroOptimisation)



In this picture the performance of the TCF is shown to remove the signal tail without modifying the pulse and die amplitude.

BSC2

The second baseline correction is only applied during the acquisition of an event and corrects non systematic signal perturbations. It is realised as a moving average filter. The correction is calculated by using the average of eight pre-samples which are in the acceptance window. The acceptance window is defined by a configurable double threshold scheme. If the next sample is outside this window it is not used to update the moving average value. This means, that if there is a big variation which is normally induced by a pulse of a cluster the correction value stays on the value which was calculated with the last sample in front of the pulse. After the pulse, the samples are again in the acceptance window and the correction is again calculated. In addition to minimise the influence of the pulses, a configurable number of samples can be excluded pre and post the pulse.



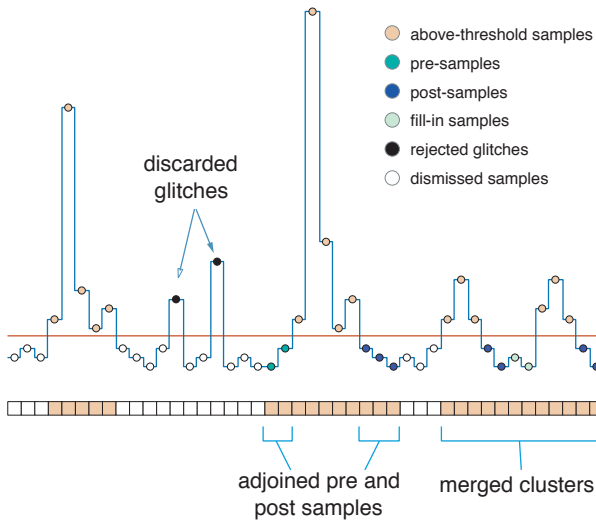
This picture shows the double threshold signal following scheme of the BSC2. During a pulse the processing is frozen and the correction value is kept.

DFU

When removing the samples in between the pulses one relevant information gets lost, the time information. As mentioned above the DFU adds two words to each sequence, the first is the time information and the second is the total length of the sequence. The time information is the time distance in number of samples after the trigger. With this additional information a decompression is again possible. In addition this unit bundles the 10 bit words to 40 bit words since the ALTRO bus has a width of 40 bit. When the last 40 bit word is not completely filled the hexadecimal pattern 0x2AA will be added as often as needed to complete this word. Finally the trailer word with a length of 40 bit is added. It consists of the total number of 10 bit words before and the "Hardware Address" which is unique for each ALTRO-channel in one readout partition (see rcu/readout), the unused start is filled with the pattern 0x2AAA and in between the numbers a 0xA.

	40	30	20	10	0
	S05	S04	S03	S02	
	S10	007	T06	S06	
	005	T12	S12	S11	
⋮					
	S91	S90	S89	S88	
	2AA	007	T92	S92	
40-bit data words	2AAA	# 10-bit w	A	Hard Add	
Trailer word					

This schematic shows the ALTRO format packing. "S" means Sample, "T" means the time position and the number the complete length of a sequence.



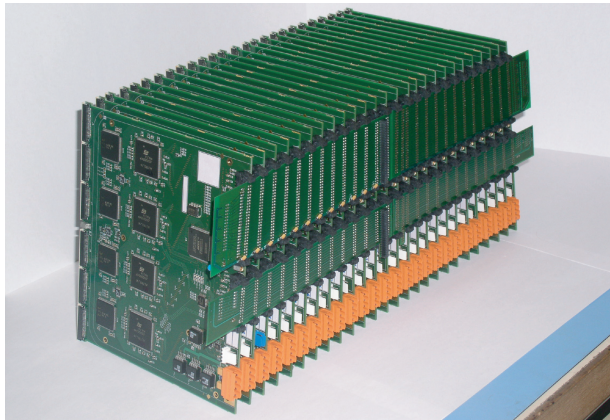
Here the behaviour of the ZSU is shown, it is configured to remove glitches of the length of one ADC above threshold.

MEB

To reduce the dead time, the data transfer is decoupled from the data acquisition of the detector electronic. For this purpose the ALTRO has a memory of 1024:40 bit and can be blocked in two, four and eight blocks. On arrival of a level one trigger the acquisition of an event is started and will be stored in the memory, if a level two trigger arrives the event is frozen in the memory and stays there until a CHRDO (Channel Readout) command is sent [n5]. If after a level one trigger again a level one trigger occurs, the memory will just be overwritten by the next coming event. With this scheme the FEE can cope with bursts of events by filling up the buffers faster than the read out, which then catches up when the event rate is smaller.

Backplane

The ALTRO-bus from each front end card is first connected to the two backplane PCBs. The backplane also delivers the termination support for the bus. For each patch in one TPC sector there is a different backplane due to the fact, that the number of FEC is differing. There are always two branches.[n1, n14]



Both backplanes fully equipped with FEC are shown. The connector to the RCU is in the middle and the termination is on both ends.

RCU

The RCU (Readout Control Unit) [n10,n15] is connected to the two branches of the FEC and has connectors for two daughter boards which are the later explained (SIU and DCS Board). The RCU provides the bus termination. The purpose of the RCU is to be the interface in between the FEE and the DAQ (Data Acquisition) and DCS. There is a ALTRO Module for the communication via the ALTRO bus with the ALTROs and the Board Controller. For the communication via the I²C link to the Board Controller there is the slow control module. The read out data is prepared by the Data Sampler to cope with the needs of the SIU. The control over the RCU is handled by the DCS card which needs three interfaces. One is the configuration of the RCU FPGA itself, to change the firmware on updates and failures induced by single event upsets. There is the interface for the DCS system to control and configure the Front End and to the TTCSR (TT:Trigger and C:Controll and Rx:Reciever) which delivers the different Trigger information [n16]. Parts of the Trigger information have to be delivered to the SIU to build up the DATE (Data Acquisition Test Environment) event header.



Here the prefinal RCU with both daughter boards (SIU & DCS) and connected on the backside the backplane with two FEC is shown.

SIU

The SIU (Source Interface Unit) is the detector end of the DDL (Detector Data Link) which is then connected to the ALICE DAQ system. The SIU uses a 32 bit half duplex data bus for the interface from the RCU and an optical transceiver to the DDL.[n16]

DCS

The DCS (Detector Control System) daughter Board is running a complete embedded LINUX called μ Clinix [n12] on an ARM 922T [n11] hardwired logic on an FPGA. This is the end of the DCS system for the TPC, so this board handles then the configuration of the FEC and the RCU and also the control of the status of the boards. The Trigger receiver is also located here. It delivers the L1 and L2 trigger information to the FEE.[n16]

Jitter

Jitter

Each clock has a certain amount of jitter, which means that the period in between two clock pulses is not exactly constant. For digital circuits this is no problem since all components are running in sync with the clock, but when working with analog signals the inaccuracy in the knowledge of the exact time position leads to an inaccuracy in the measurement of the signal, because the time point when measuring is not exactly known. The clock accuracy is a trade off between the needed time accuracy of the measurement and the effort to build the clock. Since in this case the clock is needed on all FEC on the TPC a complicated clock scheme is complex and expensive. To find out the needed accuracy a simulation was done. This simulation is described and the results are shown in this chapter.

Simulation

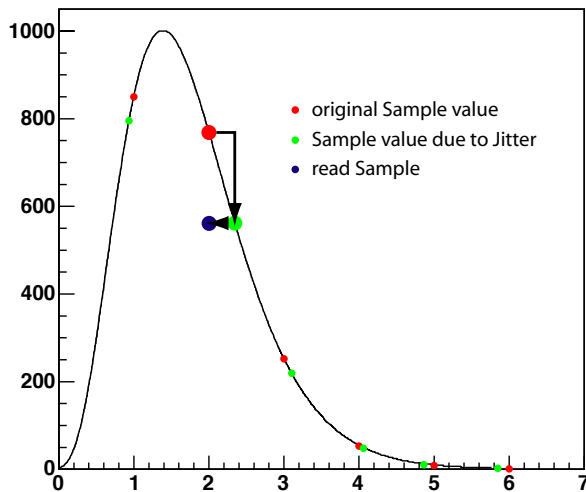
The starting point is the signal generated by the PASA, which has the shape of a gamma4 function.

$$f(t) = \begin{cases} k \left(\frac{t-t_0}{\tau} \right)^4 \cdot e^{-4 \frac{t-t_0}{\tau}} & t > 0 \\ 0 & t \leq 0 \end{cases} \quad (f14)$$

with the parameters t_0 as the starting time τ as the relaxation time and k is defined as:

$$k = Ae^4 \quad (f15)$$

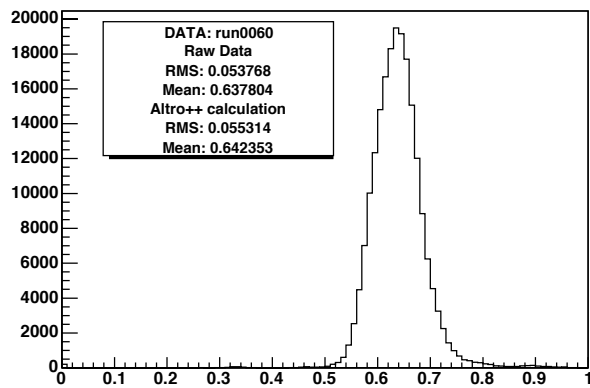
with A as the amplitude. The four is in both cases the order of the function which is defined by the PASA. This function as shown below is sampled without jitter and sampled at slightly different positions to simulate the jitter, which results in a amplitude error.



The generated signal (black line) the correct sample, the due to jitter disturbed time position and the read sample are shown.

On this values the noise of the ALTRO is added. The noise was extracted from the data recorded for the pedestal cal-

culation. For each channel the RMS (Root Mean Square) was calculated and all are collected in the plot shown below.



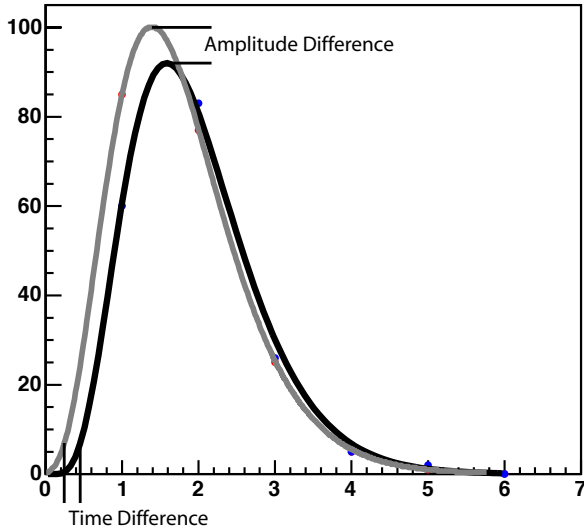
Noise spectrum of the ALTRO, the mean RMS value is 0.6.

This leads to simulate the noise using a gaussian probability distribution with a σ of 0.6. The jitter is simulated using also a gaussian distributed noise generator with a varying width which represents the assumed clock accuracy. To circumvent systematic errors by using always the same starting position t_0 it is also randomly varied. All parameters are shown in the table:

Parameter	min	max	comment
A	25	1000	20 steps
t0	-0.5	0.5	flat random
tau	1.5	1.5	fixed
jitter	sigma = 0	sigma = 2ns	gaussian random
noise	sigma=0.6		gaussian random

Parameters of the simulation

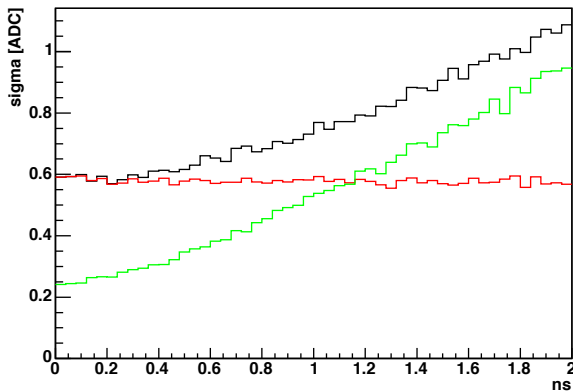
This three sets of samples: only noise, only jitter, noise and jitter are then rounded to integer values to add the quantisation noise and fitted separately using the same function as fit function. The start parameters for the fit are the original values of the generated Pulse. There are two important parameters of a cluster, the time position and the amplitude. To measure the impact of the jitter the difference of the cluster parameters of the original pulse and the disturbed one are calculated as shown.



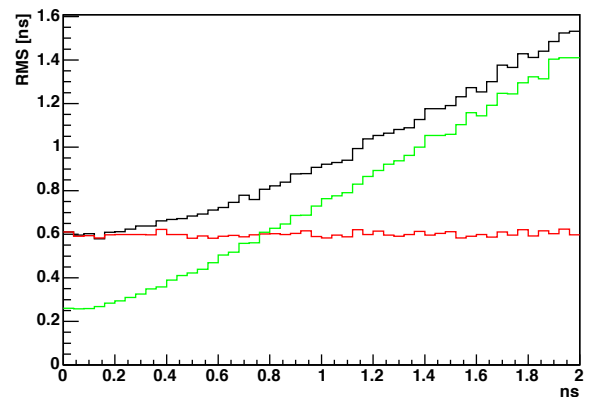
Here the generated pulse and the to the distorted data points fitted pulse is shown.

Result

This two values of 2000 different sets of pulses generated as explained are collected and from this distribution the RMS is calculated. For the amplitude difference the distribution is fitted by a gaussian to get more stable results, since when the fit is not converging this leads to big differences. The Plot below is showing the introduced error when increasing the amount of jitter by widening the σ of the random generator and a fixed amplitude of 100 for the amplitude precision and below for the time accuracy. The red lines shows the influence of the noise alone, the green of the jitter alone and the black of both. As expected the noise introduces a constant error and the error of the jitter increases with the decreasing accuracy of the clock.

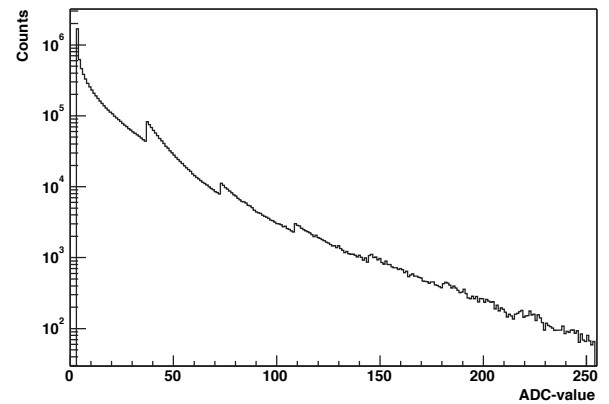


Difference in the amplitude measurement with increasing amount of jitter. Red is the influence of the noise only, green the influence of the jitter alone and black is the combination of both.



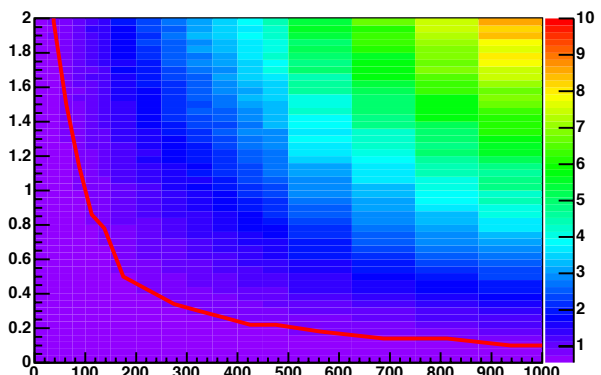
Difference in the time measurement with increasing amount of jitter. Red is the influence of the noise only, green the influence of the jitter alone and black is the combination of both.

The ADC value of a cluster in the TPC data is less probable the higher the value is. This is shown in the plot below:

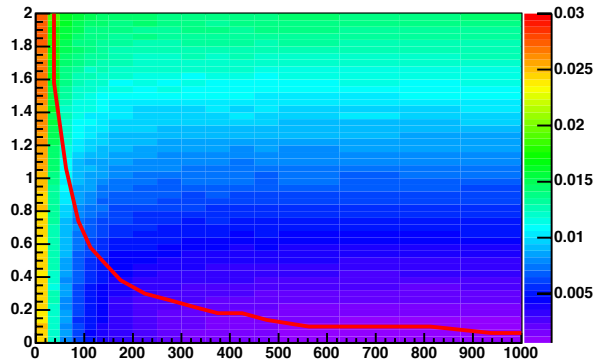


Distribution of the ADC values in an simulated event of the TPC (ref anders)

The simulation was done for 17 different amplitudes from 25 to 1000. The results are shown in the two plots below for the amplitude error and the time error.

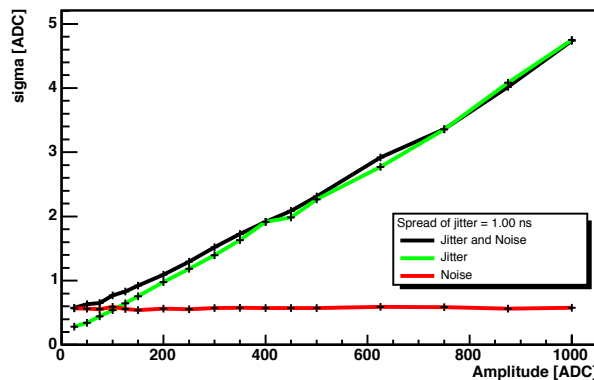


Difference in the amplitude measurement through all simulated amplitudes and jitter. The red line indicates the crossover in between the noise and the jitter as main error source.

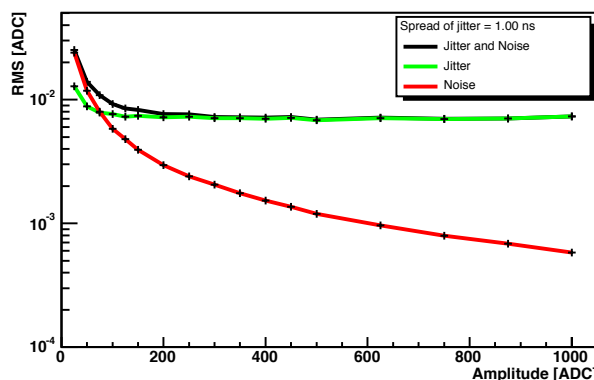


Difference in the amplitude measurement through all simulated amplitudes and jitter. The red line indicates the crossover in between the noise and the jitter as main error source.

The red line indicated the crossover in between the noise as the dominant source of the error and the jitter.
In the following two plots the cut along the foreseen clock inaccuracy of 1 ns is shown.



Difference in the amplitude measurement at the foreseen clock accuracy.



Difference in the time measurement at the foreseen clock accuracy.

Prototype Environment

Prototype

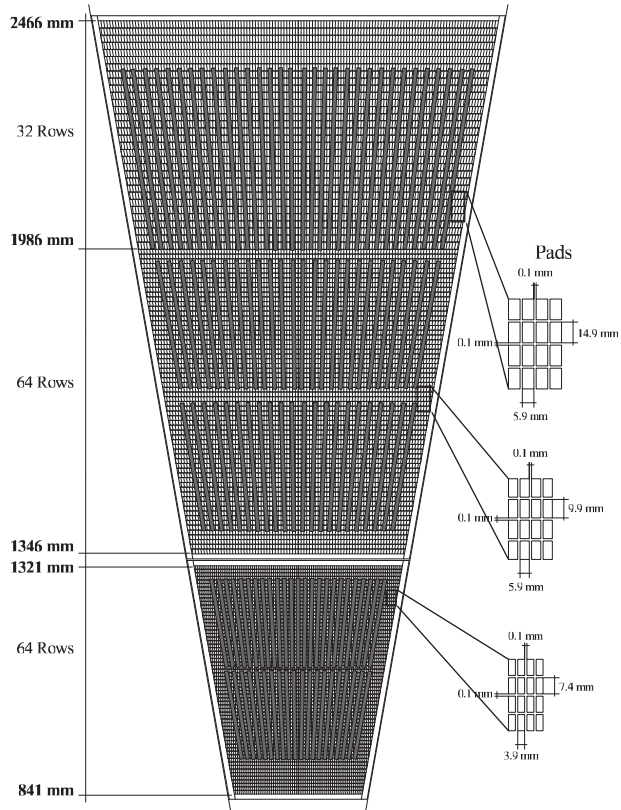
A small prototype was build to do a TPC performance test. It consists of one IROC (Inner Readout Chamber) module on one side and a complete fieldcage with a central membrane in a gas tight aluminium box. First tests were done to verify the electrostatic behaviour without a readout system. Later for the complete TPC performance test, it was equipped with four FEC boards and a cosmic ray triggering setup using scintillators. At this time the front end cards were uncooled and the test TPC was flooded with ArCO₂ gas mixture. Later a simple cooling setup and four additional cards were added and the gas mixture was changed to NeCO₂. The cooling system is based on a underpressure liquid cooling and a copper shielding around the FEC as shown in the FEE chapter. This setup was used to gather some statistics of cosmic particles on MIPs as the most probable particle, showers as an estimate for the high multiplicity environment and particles with a big ionisation to see saturation effects, as also since two different gas mixtures were used to study differences in the signals. The data is available at [n21]

length	2.7m
diameter	1.1m
drift length	1.35m
Anode Voltage	1245V
Fieldcage Voltage	55.8 kV (400 V/cm)
Gas Mixtures	90% Ar 10% CO ₂
	90% Ne 10% CO ₂
	90% Ne 5% N ₂ 5% CO ₂

Detector Parameters of the test TPC

IROC & Mapping

The endcaps of the ALICE TPC are circular and parted in 18 trapezoidal segments on each side. The pad plane follows this scheme and is subdivided in two parts, the IROC and OROC (Outer Readout Chamber) as shown in the scheme in the next column. Another subdivision is given by the ordering of the FEC, there are six rows of them, two on the IROC and four on the OROC, this subdivisions are called patches. Due to this trapezoidal form so different number of pads per row a trivial direct mapping of the pad to one readout channel is not possible. Each pad has an unique number per ROC (Readout Chamber), starting with 0 as the left pad in the innermost row and then counting every pad until the outermost row. A table of the pad index correlation to pad and row, FEC, cable, connector and pin for the IROC and OROC exists.[n18]



Distribution of the FEC on the Readout chamber. Both the IROC and OROC are shown.(IROC+OROC in pic)

Data Acquisition and Configuration

The data was read out via the ALTRO bus with an old version of the RCU often called RCUI via a flat cable. This version was based on a commercial PCI (Peripheral Component Interconnect) card, a board from PLDA [n1] with an FPGA and a commercial PCI core also from PLDA [n2]. In addition there was a mezzanine card put on top of the RCUI to interface to the ALTRO bus. The host operating system was LINUX [n20] with a low level PCI driver to interface to the RCU. The registers of the firmware in the FPGA were mapped in the address space of the computer. A set of small C [n3] routines handle the communication to the driver as also the coding and decoding of the readout memory (->altroFormat). This C routines are interfaces with a LabVIEW [n4] based GUI (Graphical User Interface). The LabVIEW software also implements the control, setup logic, graphical displays of the running status and storing of the data. The choice of LabVIEW determined the data format and the speed of the acquisition. The speed was limited to roughly storing 2 MByte/s with the equivalent of an 1 Hz event rate, since the trigger rate for cosmic, especially when adopting the trigger to select high multiplicity or high ionisation events the speed was sufficient. The data format as described below is big endian. There is the historical approach of building little endian systems which means they are working in low byte high byte order, since this approach needed less transistors. Outdated CPU architectures like x86 (for the Intel IA32 line and AMD Intel compatible line in 32 and 64 bit) the Intel Itanium and the Digital Alpha are using this scheme.

And there are the big endian systems, which are working in order, so high byte low byte. This scheme is more efficient in handling integer data. Most CPU architectures are following this paradigm like the IBM and Motorola PowerPC platform, SPARC and MIPS. Since LabVIEW has its origin on big endian systems they use only this format when writing binary data independent on the hosting platform. When reading this files with another program or programming language on a big endian system there is no problem, but when reading them on a little endian system the byte order has to be swapped as described in the following table.

length	C++ name	Big Endian	Little Endian
1 Byte	char	B_0	B_0
2 Byte	short	B_1, B_0	B_0, B_1
4 Byte	long int	B_3, B_2, B_1, B_0	B_0, B_1, B_2, B_3
8 Byte	long long	$B_7, B_6, \dots, B_1, B_0$	$B_0, B_1, \dots, B_7, B_8$

Table showing the difference in the big endian and little endian coding.

Data Format One

The first data format is in principle no format, as the data is just written as a continuous stream of the samples in one channel as big endian coded short integers (16 bit) numbers and increasing ALTRO address. Without the knowledge of the configuration as number of samples per channel and number of channels, which are not included in the file the data is not decodable.

Data Format Two

The second data format added a header in front of the data, which is then saved as the first format. The header consists of the number of channels, the list of active channels, again the number of channels, the number of samples per channel and the data block. The double number of channels is only because of the way LabVIEW stored the data. In the header short and long ints (32 bit) are used.

	Format 1	Format 2
#channels	-	long int
channellist	-	#channel * short int
#channels	-	long int
#samples	-	long int
data	$n * \text{short int}$	$\# \text{channels} * \# \text{samples} * \text{short int}$

Data formats of the LabVIEW based readout Software

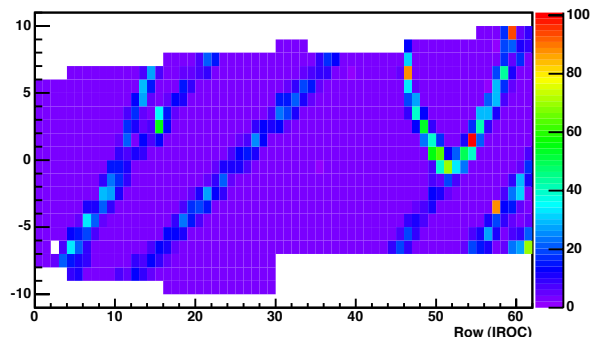
Monitoring

In this set a quasi online monitoring system was integrated to offer a way for a fast visual inspection of the data. Implementing a monitor by using LabVIEW would introduce a number of drawbacks like low speed, high complex-

ity in debugging, complicated maintenance and expensive, since it would depend on a commercial product. As platform for the monitoring ROOT [n5], a well known data analysis framework was chosen. A set of C++ [n6] classes were developed to have a fast data decoding and analysis and packed in one .so (Shared Object). The interactive part is based on a set of CINT (C Interpreter) [n7] macros which call the functions and classes of the .so. This adjudication of extending ROOT with the needed classes made the monitoring package independent on the running platform, as long ROOT is available [n19]. Since the online monitor was running in the interactive mode of ROOT all plot manipulation capabilities are available as well as the save functionality. The monitoring was working on an request base, so the user requests a new event, the newest stored file is read and then displayed.

As stated before the data is stored in the readout order which means that starting from FEC to the last and in each FEC the channels are sorted in ALTRO addresses. Since there are four ALTROs on each side and the connection lines to the PASA are optimised to be short, the addressing on the top side is in FEC-channel order and the ones on the back-side in the reverse order. This internal ordering was added to the mapping table of the IROC. The pad index was replaced by the channel number in readout order (appendix table). Unfortunately this means that every configuration of FEC equipped needs another mapping table. In the picture below the topview of the maximum ADC value of each channel of the eight FEC on the test TPC is shown.

Event: "/Volumes/TPCData/RUNS/run0052/evt0129" Timebin: 0-999

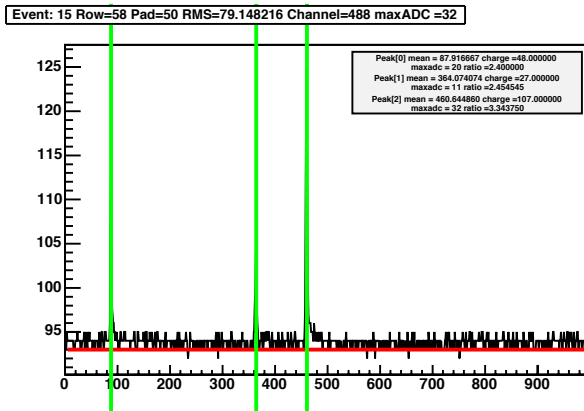


Topview of a cosmic event of the test TPC equipped with 8 FEC.

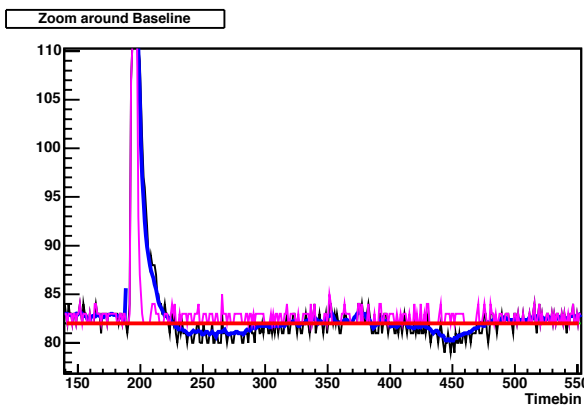
To get a useful topview of the TPC there were two methods to calculate the baseline, one online and one offline and subtract it from each channel. The online version is based on a double pass calculation, the first pass calculates the mean over all timebins regardless on the variance, the second pass then sets a double threshold scheme around the previously calculated baseline and recalculates it only using the samples inside the window. For low occupancy events this approach provided results with a negligible error compared to the offline version. The second called offline method favours a special pedestal run or uses a normal data run. When having a pedestal run, the mean of each channel is calculated and then averaged over all events and stored. The scheme is slightly more complex when having no special run. Then only channels without

a signal are used for the calculation, which was possible since most cosmic events had a very low occupancy. The pedestals were stored in the format readout number and pedestal. (LTstability?)

From the topview the channel view was accesible by just moving the mouse over the pads. As soon as a new pad gets the focus the channel view was updated with a maximum rate of more than 10 Hz. In the channel view the baseline, a moving average calculation, the ALTRO++ calculation (->ALTRO++) and a pulse finder as also a zoomed view around the baseline to study the signal tail was available and configurable.



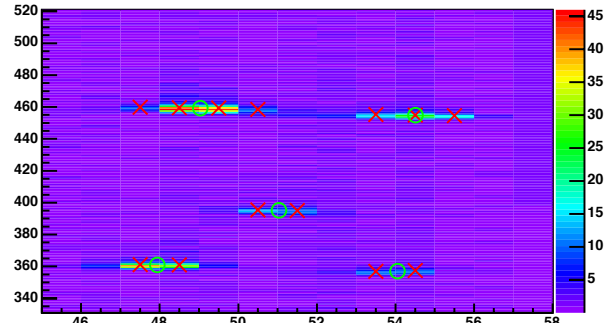
Pad view of a cosmic event. The black line is the signal, the red line is the baseline, the green lines are at the position of the weighted mean of the peak. In the grey box the parameters of each found peak are shown.



Zoomed view of a pad of a cosmic event. The black line is the signal, the blue line is the moving average and the pink line is the ALTRO++ simulation.

When clicking on a pad and holding the button, the pad view was frozen to keep the wanted pad to allow to modify the plot like zooming or fitting the signal or saving the plot as eps, ps, svg or gif (eps: Encapsulated Postscript, ps: Postscript, svg: Scalable Vector Graphics Format, gif: Graphics Interchange Format).

On a double click the row view was opened. Here the ADC are displayed color coded, a cluster finder was available, both the centroids of the pulse finder in each channel and then the merged cluster were displayable.



The configuration was splitted in two files, one for the configuration of the monitor behaviour, like screen resolution or the configuration of the moving average display and the other for the run related parameters like the path to the run files or the pedestal files. in appendix ?

As an independ entity there was a macro which could draw a 3D representation of the ADC in the event. This used the OpenGL (Open Graphics Library) [n8] capabilities of root which allowed to zoom, move and rotate in real time.

Test Beam

This year in spring there was a beam test with the described setup in the PS (Proton Synchrotron) testbeam, but fully equipped with FECs and cooling as well as the use of the gating grid during data aquisition. Since the test beam was also seen as integration test of the complete data and trigger chain a preversion of the final RCU, the DCS Board a DATE detector readout and a small Trigger setup were used. The previously used flat cable was exchanged by the current version of the backplane. This amount of changes had a big impact on the software needed to configure, control and monitor the TPC. The TPC gas was changed to the final ALICE choise of Neon Nitrogen CO₂. In addition to the TPC there was a silicon telescope and a TOF detector present and included in the trigger and data aquisition system.

Configuration

The configuration of the front end electronics is completely different compared to the previous setup. The prior setup with a PCI based RCU has changed, there are now two paths to the RCU, one is the DDL via the provided low level communication library and the FeC2 (Front End Control and Configuration) script language for easy development and debugging data transfer [n9] and a ethernet connection to the DCS board. The internal communication layer of the DCS board and the steering host above is based on the DIM (Distributed Information Management) client server system and is called InterCom Layer [n10]. Its foreseen to implement the InterCom layer also over the DDL to get the same acces via the different physical layers. This will replace the FeC2 script language or the low level

DDL communication library which have no user C/C++ interface.

Readout

The readout is now done via the DDL and the DATE system, which made a new online monitoring scheme necessary. When the electronic is set up the data aquisition is started. There are two patches in one IROC so also two RCU cards and two DDLs for the aquisition system. The data of this two links as well as the data from the silicon telescope and the TOF are then merged in one DATE file.

Data Storage

During this test beam roughly 0.5 TB of data were taken. This data was firstly stored on the local discs of the DATE computers at the experiment and then tranfered to CASTOR (CERN Advanced Storage Manager) a CERN central taping system for the LHC data [n22,n23]. Irritatingly off site access to the data in CASTOR is complicated and insecure.

Data Format

The usage of DATE as readout system also introduced a complete new data format as well as the usage of the new RCU, which introduced the final ALTRO format. Each RCU reads out both branches of one complete patch and converts this 40 bit data into 32 bit data since the DDL only supports this. This is done as shown in the scheme below.

31	24	16	8	0
ALTRO WORD1[31..0]				
ALTRO WORD2[23..0]		ALTRO WORD1 [40..32]		
ALTRO WORD3[15..0]		ALTRO WORD2[40..24]		
ALTRO WORD4[7..0]	ALTRO WORD3[40..16]			
ALTRO WORD4[40..8]				

Translation scheme to convert 40 bit into 32 bit by the RCU data sampler.

So four 40 bit ALTRO words are converted in five 32 bit words. Ahead this data block a header is added which is similar to the standard DATE event header. The header consists of seven 32 bit words and is shown below.

31	24	16	8	0
Format Version [24-31]	L1 Trigger Type [16-23] (1)	Res. MBZ	Event ID 1 (Bunch Crossing) [0-11]	
Res. MBZ			Event ID 2 (Orbit Number) [0-23]	
Block Att.[23-31]			Participating Sub-Detectors[0-23]	
Res. BZ	Status & Error Bits [12-27] (2)		Mini-Event ID [0-11] (3)	
	Trigger classes [0-31] Low (4)			
ROI L. [28-31]	Res. MBZ. [18-27]		Trigger classes [0-17] High	
			ROI High [0-31] (5)	
ALTRO CHANNEL 1 DATA (6)				
ALTRO CHANNEL 2 DATA (6)				
.....				
ALTRO CHANNEL n-1 DATA (6)				
ALTRO CHANNEL n DATA (6)				
Event Length (7)				

Complete data block generated by one RCU at the test beam. The blue entries are set, the black ones are fixed to zero.

At the end the total number of 32 bit words is added, this is extremly important because its needed to retranslate the 32 bit data back into 40 bit. This shown block is callees “payload” in the DATE language.

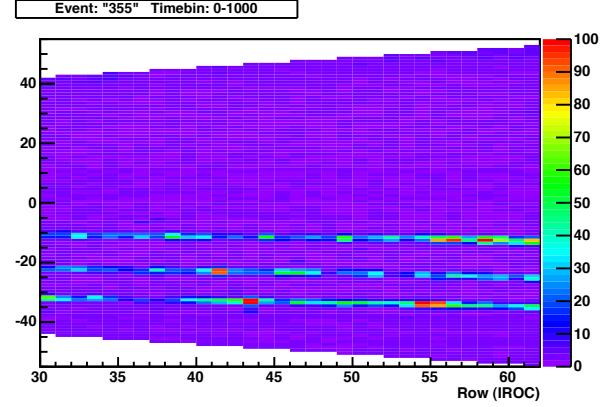
From the RCU this data is transferred via the SIU into the DATE system which collects the data from all different sources and merges this to one event. DATE collects several events in an quite unhandy file format by just concatenating them in the event number order. Each event starts with an event header composed of the GDC (Global Data Concentrator) which consists of the total event size the event id, the event type, the run id and other by DATE used informations. Importand is the event id, since there are certain types of events without physical relevance, which have to be excluded from any analysis or monitoring. After the event header a sub event header follows, which includes the information coming from the first LDC (Local Data Concentrator) which finished the data transfer. Now the equipment header follows, it consists of the equipment id and additional data of each DDL, since it is possible to have several DDLs with one LDC as target. Now finally the previously described data block is concatenated. In the case of the test beam there were both DDLs plugged in one LDC, so after the first data payload the next equipment header followed with the data block. The equipment id is used to identify the different RCUs so the different patches of the TPC, it is a integer number and unfortunatly the meaning of each number is nowhere included in the files and also no fixed definition exists, so to decode the data it is mandatory to also know the exact setup of DATE. If there are additional LDCs in the setup a new sub even header is concatenated with the previously described equip-

ment header and data payload. The information of how many equipments are coming after each sub event header is stored nowhere, so no crosscheck of the event structure is possible. At the testbeam there were two additional LDC one for the silicon telescope and one for the TOF. In the files the order of the LDCs is mixed since as described above the first finished is the first stored. Irritatingly also in the event header the number of following sub events is not stored. The only way to get back on track if an error is in the event structure would be by scanning for the event magic number in the event header which is fixed and in principle used to identify if a endiannes swap happend. Irritatingly this sequence can also occur in the data so this method is insecure. In the DATE files aquired during the test beam some do not have a correct structure. All readable events up to the point of the uncorrect structure are used and the remaining events are discarded. At last in an event file nowhere a pointer to the included events or even the number of the events is stored, the complete event has to be parsed to get this information. It would have been a trivial task to concatenate this information at the end of the file. scheme of format

Monitoring

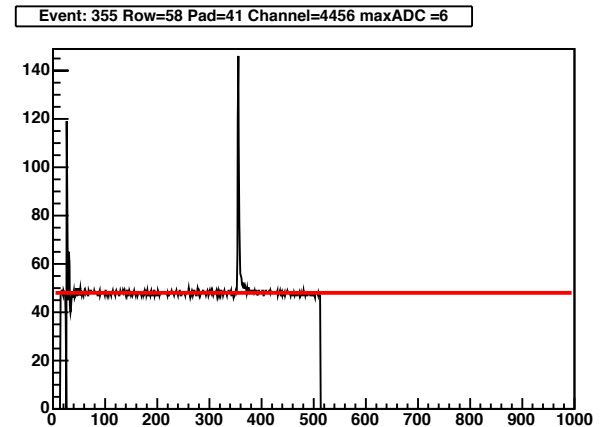
Plenty of changes and new implementations were needed as also backporting to an completly outdated operating system (Red Hat 7.3) and non standard compiler (gcc 2.96). At first the idea of having the written event files as interface was not possible anymore, since the DATE group did not want this simple approach. Now there are two running modes in the online monitor one uses a DATE library to access the data online and the other one which reads stored DATE files. Irritatingly there was neither a library nor a class which encapsulates the interal DATE format which is roughly explained above [n11, n12] and also the availabe documentation was outdated and incomplete. Several C++ classes were implemented to get an encapsulation of the monitoring library and of the file access. Based on this a class to encapsulate the DATE format was implemented, it uses a slightly modified version of the provided event.h header file to decode the header and gives access to the data payload and the included information in the header. The change in the header file was neccassary due to an incompatibility with CINT.

The online monitor extracts the two data blocks of each RCU and first translates the 32 bit into 40 bit which are stored in 64 bit integers and then decodes the internal ALTRO data. At the moment the RCU firmware does not include the branch number into the ALTRO address, so there every address is doubled. This is cured via the AltroFormat class which searches for a falling edge to find the crossover point in the branch and then sets the twelfth bit to code the branch. Both encoded data blocks are then merged and the double addresses are eliminated setting the patchnumber at the thirteenth bit. This can also be extended for more patches by the usage of higher bits. In the mapping the readout count number was exchanged with the patched ALTRO address which is now unique for each channel.



Topview of an test beam event of the fully equipped test TPC. The beam is entering the TPC from the left. REDO

Another change is visible in the pad view. There are always 12 samples at zero in the start, this is due the length of the processing pipeline of the ALTRO [n14]. Additionally the length of each channel is not known, this is set at the time when the ALTRO is configured. Since this is done manually and independent of the data aquisition so this information is stored nowhere. The structure in the beginning of the channel is induced by the switching of the gating grid.



Pad view of a channel from a test beam event. The first 12 samples are zero due to the length of the processing pipeline of the ALTRO. The aquisition length was configured to 500 timebins. The structure in the start is induced by the switching of the gating grid.

This information could have been extracted from each ALTRO coded channel as long the zero suppression is turned off. It was forseen to also take data including the zero suppression but there were problems in configuring all channels with the correct baseline which is mandatory. There is a monitoring sub system from the DATE group which was not available during the test beam since it could not handle the TPC data and also the scheme to implement the monitoring of the data in the data aquisition system is questionable.

HLT

In the testbeam also the HLT was included as a data receiver and also producer. The HLT gets the data payload of both RCUs. In the HLT publisher subscriber [n15,n16,n17] system for the data processing the AltroFormat class was included to decode the ALTRO data. Unfortunatly during the test beam there was not enough time to also complete the monitoring to run as a HLT client.

ALTRO Parameter Optimising

Parameter Optimising

The digital processor of the ALTRO has to be accommodated to the detector response of the ALICE TPC by configuring the different processing units in the digital processor. For each of this units a different scheme to extract the parameters has to be used. Since the effects of the processing are not completely reversible it is important to have a good crosscheck of the influence of the parameters on the data and the wanted impact during the extraction.

BCS1 Parameters

Depending on the working mode [n12] the BCS1 processing part of the ALTRO needs to be configured with a correct pedestal pattern and an overall baseline for the channel. The extraction of the fixed baseline is described in the previous chapter. To extract the pedestal pattern a similar approach was chosen, so all channels which have a signal at a time after the gating grid effect are discarded. All accepted channels are divided into their timebins and each ADC value is stored in an data array of the dimension channel and timebin as also in a different array of the same dimension, the count of found valid ADCs per channel and timebin is saved. After processing all events the mean of this values is calculated and stored with the in ->Prototype described extended hardware address as unique identifier. The configuration process to finally send this look up table to the ATLRO is described in this chapter in »Computing«.

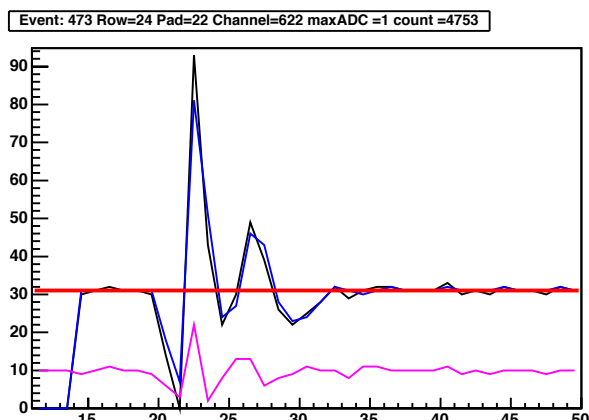
Extraction

Based on a run taken at the TPC testbeam the look up table was computed. At this step several problems occurred with the integrity of the stored data. A few data files weren't completely written by DATE so the event structure was inconsistent, these files were discarded. The more severe problem in many runs was that the hardware addresses of the read out ALTROs had errors. Three check criteria were implemented. The first check just verifies that the read hardware address is smaller than the biggest allowed one. This check is more important for the implementation of the mapping table, since this is a boundary unchecked array, as usual in C/C++, and accessing a non existing position causes a crash of the program. The second check verified that the read hardware address is valid, so it is in the predefined set of addresses of the IROC module. The third check verifies that each address is unique. When a doublet is found the event is checked again in reverse order to find the second address of the doublet. The error log of run 820 is attached in the appendix as an example. To create a pedestal pattern a correct mapping is mandatory, so all events which have at least one error are discarded. The reason of this hardware address problems is most likely located at the RCU firmware level, since there was only a small amount of time to implement the firmware on the new RCU hardware before the start of the testbeam. Timing problems in the FPGA code could easily generate errors like this. These

problems are currently investigated at the FEE group at CERN [n1].

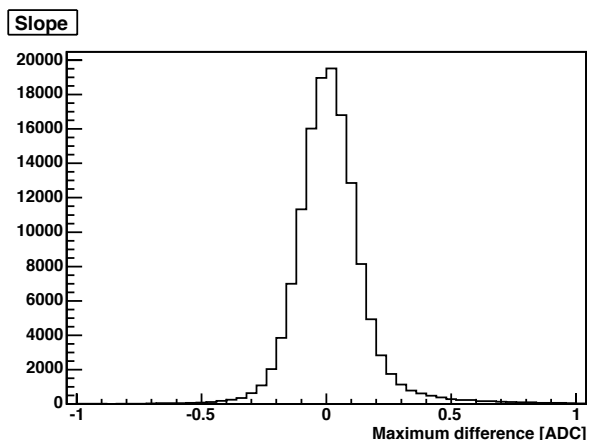
Result

An interesting part of the signal is the influence of the gating grid switching, this should be a systematic effect and constant over time. The plot below shows the signal, the corresponding baseline pattern and the result of the correction.



Signal of one channel. The black line is the ADC data, the blue line is the corresponding pedestal LuT, the red line is the fixed pedestal and the pink line is the signal after LuT subtraction. For a better visibility an arbitrary 10 was added.

The influence of the gating grid switching is substantially decreased but not completely removed as shown in the plot above. To get a general overview of the correction capability on this data the instability of the data was analysed. Firstly each timebin of each channel over all events was fitted with a line to observe possible baseline variations over the time. In the plot below the maximum time dependence of the timebins past the influence of the gating grid is shown.

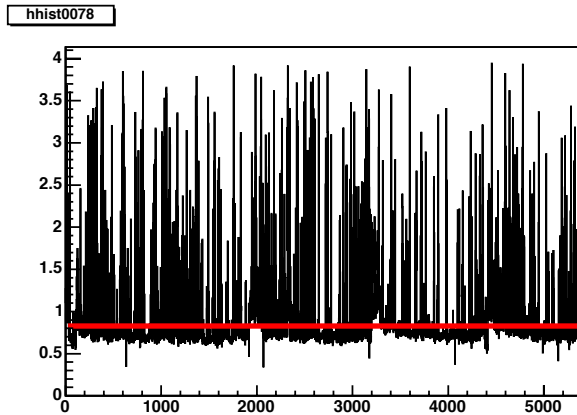


Maximum dispersion of the basline over the total acquisition time of this particular run. (run 820)

It leads to no relevant difference, since mostly every slope leads to a maximum difference below the quantisation noise level.

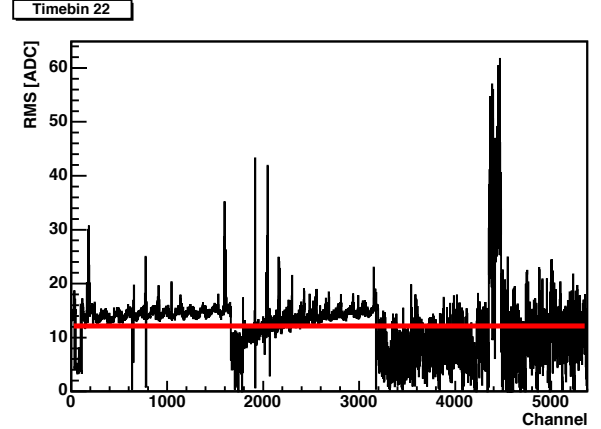
Baseline Dispersion

Secondly the dispersion of each channel and timebin over all events was calculated using the RMS. Only channel, timebin doublets with a small inner noise can be sufficiently corrected by the use of the LuT. For the time domain of the signals past the gating grid influence this inner noise is sufficiently small and therefore the baseline is correctable. In the region influenced by the gating grid the effect is not completely correctable, since the inner noise is beyond the correctable limits. In the plot below the RMS values of all channels an the specified timebin is shown. The peaks are artefacts of signals, since this calculation was done on data with signals, not like the final approach to use a dedicated run with the complete detector and trigger only without signals inherited by tracks, called pedestal runs. The fit of the line shows that the weight of this glitches is small.



RMS values of timebin 78 over all channels. The mean value is 0.83 ADC including the visible glitches. It is expected that a pure pedestal run would have a mean value of around 0.7 ADC

In the Plot below the same inner noise is shown, but calculated at the timebin 22 which is the most influenced one, by the switching of the gating grid. Clearly a wide spread is visible, so the influence cannot be fully corrected. In the testbeam the electrical version of the gating grid pulser was not the final one as also the trigger setup, this are two possible sources of the big visible variance. Additionally the grounding of the two patches had a different quality as clearly visible at the change at channel 3328 as also the different branches of the RCUs at 1664 and 4352.



RMS values of timebin 22 over all channels. At this time the gating grid influence is maximum. The trend changes at channel 1664 and 4352 are the different branches and at 3328 the RCUs change.

As shown in the first plot the correction of the baseline using the LuT in the BCS1 is working on real data, as also the influence of the switching of the gating grid is up to a certain extend removable. Since this analysis was only based on normal data instead dedicated pedestal data and the current version of the used detector electronics the conclusion is that the baseline correction of the complete data is possible.

TCF Parameters

The TCF has six parameters to be accommodated to the real signal shape, which means that these parameters are extracted from the real detector response. In general the accommodation has to follow the working principle to shorten the signal but not to change the amplitude or create over or under shoots after the pulse.

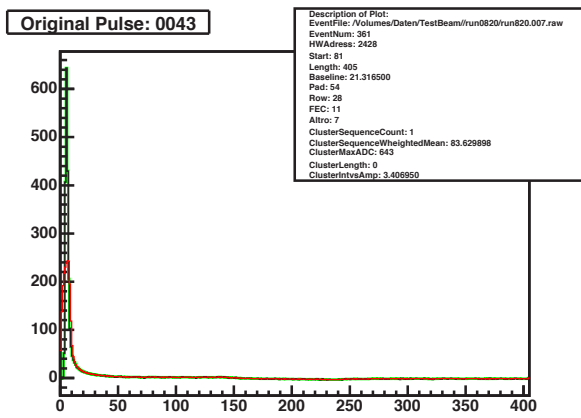
The basic fact, that the parameters are extracted from the data opens up two schemes to find a general set of parameters. Firstly to create a universal pulse by selecting pulses from the data, normalising and positioning them. From this universal pulse the parameter set would be derived. Secondly to search for the best set by extracting the optimum parameters for each pulse individually and then choosing the best working set. This path has been implemented and tested.

Pulse Finder

The first step is to find a good set of pulses. There are certain requirements at each of these pulses, they should have a sufficient amplitude, should not be disturbed by glitches or other pulses and the tail should be inside the acquisition window. Technically the chain to find these pulses starts with discarding the gating grid influenced data (discard first 12 timebins of the pipeline delay of the ALTRO and 26 of the gating grid influence), followed by the amplitude criteria. Only pulses which have an amplitude inside the set band (min: 600, max: 800) are accepted. The band should be narrow, to get similar pulses. It should accept high am-

plitudes to maximise the signal to noise ratio, but it should be smaller than the maximum amplitude (1024 ADC) to avoid overflow effects. Also only one pulse per channel is allowed to avoid crossover effects. The position of the pulse should be at small times (max position timebin 200) to have sufficient time in the acquisition window left to also include the tail. Some pulses have an extremely big integral compared to their amplitude, this can be created by several detector effects. The ratio of amplitude and integral can be limited (< 4.5) to remove this type of pulses. All remaining signals are then saved with a smoothed tail to avoid influences by the noise. The smoothing is done by a moving average calculation which starts after the pulse. All parameters are briefly described in ->Appendix.

To crosscheck the set parameters there is an additional program which reads the stored pulses and plots them into a .ps file, including the pulse information. Below an example pulse is shown.



Extracted pulse found by the pulse finder. The black line is the signal, the red line is the moving average and green is the resulting smoothed pulse. All pulse parameters are shown in the parameter box.

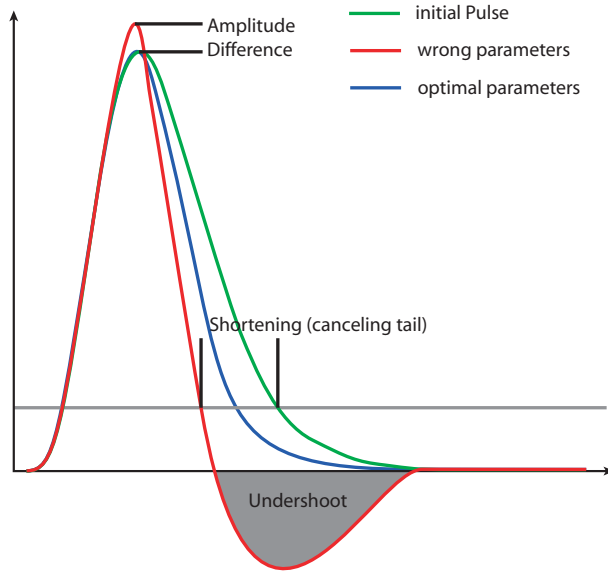
Parameter Set Finder

To derive a parameter set from a given signal a algorithm was developed and implemented in MATLAB [n3] and is described in [n2]. This algorithm was re implemented in C++ and optimised to reduce the calculation time by roughly two orders of magnitude. Each pulse will be processed and the optimum parameter set will be stored. Two stages of the TCF are used to remove the tail, the third is used for equalisation to keep the amplitude. Each stage can be individually configured in the parameter set finder.

Correlator

The correlator applies all parameter sets on one given pulse by a floating point version of the TCF algorithm of the ALTRO. The idea is to compare the optimal parameter set, so the set which was created by the parameter set finder for this pulse (optimal set), with the result of all other parameter sets of the other pulses (correlated set). To determine the difference in the resulting pulses three quality measures had been defined as shown in the plot below. The first

one is the amplitude difference in between the optimal and the correlated set. The second one is the difference in the shortening of both sets. At a configurable level the length in between the two crossing points of the application of the optimum set and the correlated set is calculated. The third one is the difference in the undershoot integral after the pulse. All this differences are stored.



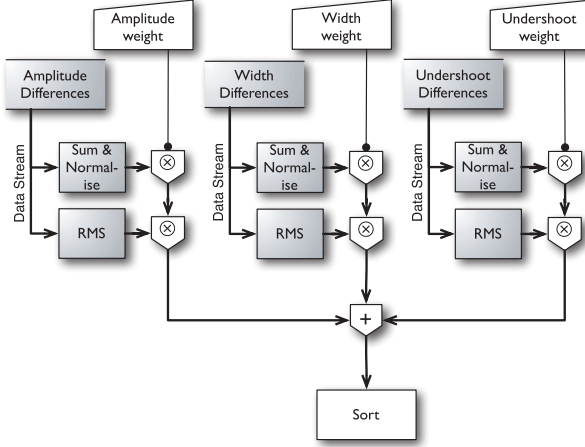
TODO FIX SHORTENING
Schematic of the three pulses with the quality measures

Best Set Finder

The final task is to find the best set. The first step is to define the wanted criteria, which is for the TCF the sustainment of the amplitude, minimising an undershoot and maximising the shortening of the tail as previously described. This is preserved by the parameter set finder. For the best set finder the criteria is that the differences in between the optimal set and all correlated sets should be minimised. In other words the search is done to find the set which works best for one pulse and works still works best on all other pulses.

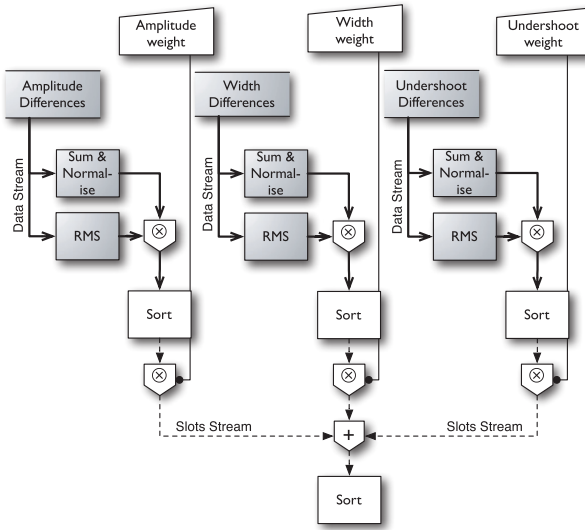
For this purpose two schemes were implemented which start from the same base as shown in the to scheme flowcharts on the next page. Firstly all differences in each of the quality measures of all correlations in between the result of the pulse with its optimum set and all results of this set with the other pulses are summed. This sum is then normalised and the RMS of all differences is calculated.

The first scheme "Weighted Quality" tries to combine this three quality measures and then find the best one. Each quality measure has a weighting parameter to vary the importance. Additionally each measure can be weighted by the RMS value to reward the set which has the most steady performance. All weighted values are then added and sorted afterwards. The result is a sorted list starting with the set with the lowest value as the best one. This scheme has the advantage to be simple but the disadvantage that the addition of the different measures is not explicit, since the normalised and weighted distributions can have big differences.



Flowchart of the “Weighted Quality“ scheme. The greyish boxes mark the common block of the schemes.

The second scheme “Weighted Vote” uses the idea of an election. Each measure can be weighted by the RMS value to reward the set with the most steady performance and is then sorted individually. There are now three uncorrelated elections of the best set for each quality measure. These elections are combined by adding the slot number of the individual elections. The set with the lowest number of elections is the best one. There are additional weights to vary the importance of the separate elections.



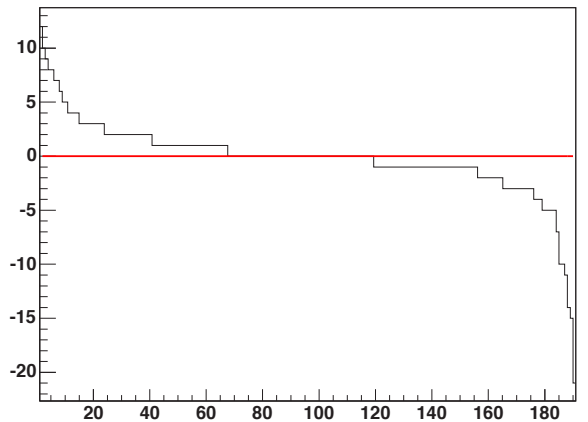
Flowchart of the “Weighted Vote” scheme. Add desc for vote streamThe greyish boxes mark the common block of the schemes. The black lines indicate a data stream, the dashed line a slots stream.

This scheme is more complex than the previous one but has the advantage that differences in the separate quality measures are replaced by a position.

To crosscheck the performance several plots are produced. As a summary for each quality measure the results are sorted and plotted. Problematic pairs of set and pulse are then on the left and right due to their big difference to the optimum set. An indication that the best set is not working well is when the extreme ends are strongly populated, translated this means that the set works on many pulses

quite well but does a lot of harm to the rest. The next step is to inspect the pulses, since the reason of this behaviour can also be that there are strange pulses found. This pulses should be removed and then the calculation has to be started again with the parameter set finder.

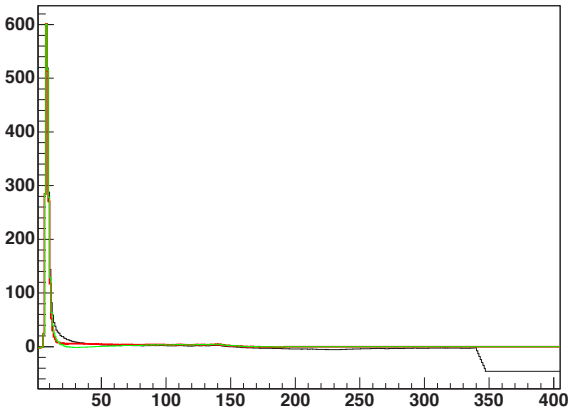
WidthAbsSetNr:0011



Example quality plot for the shortening amount. Negative values indicate a lengthening of the pulse, positive vice versa. Overpopulated ends indicate a non optimal parameter set.

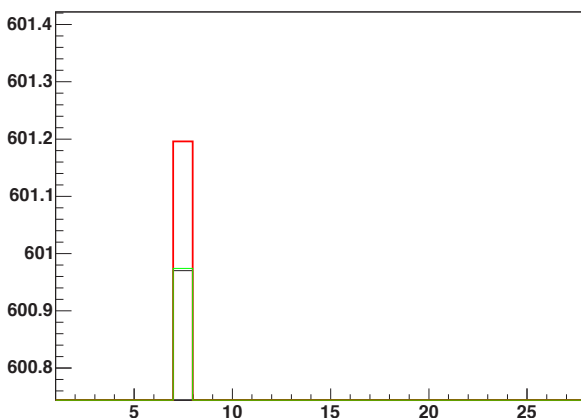
To have access to the original pulses and the results of the TCF using the optimum set of the pulse and the one which was found as the best set, a set of four plots per pulse is created. Starting with an overview of the three pulses. Followed by a zoom on each of the three quality measures.

SetPulsePos:0051

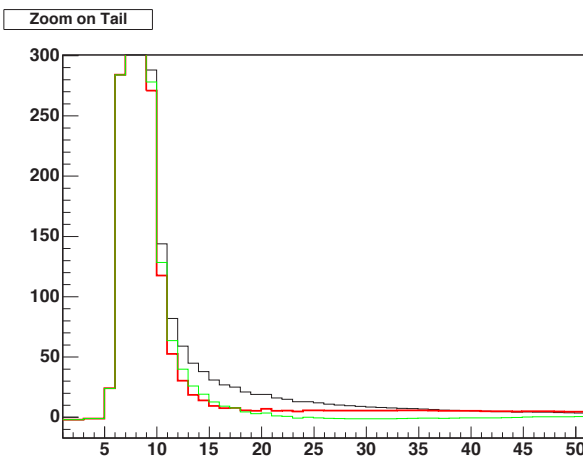


Overview over the three pulses. Black is the original signal, green is the signal processed with the optimum set and red is the signal with the correlated set.

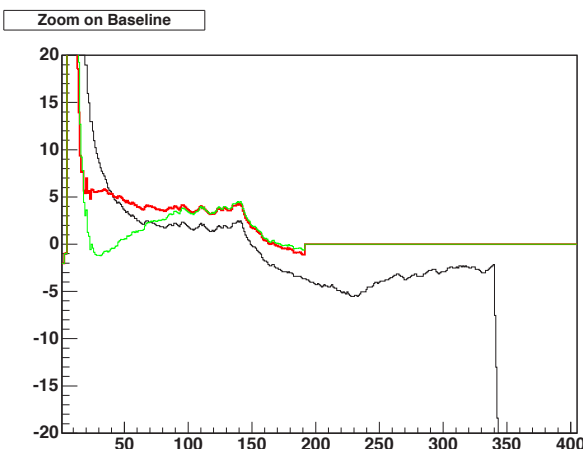
BSC2 & ZSU Parameters



Zoom on the Amplitude difference. Black is the original signal, green is the signal processed with the optimum set and red is the signal with the correlated set.



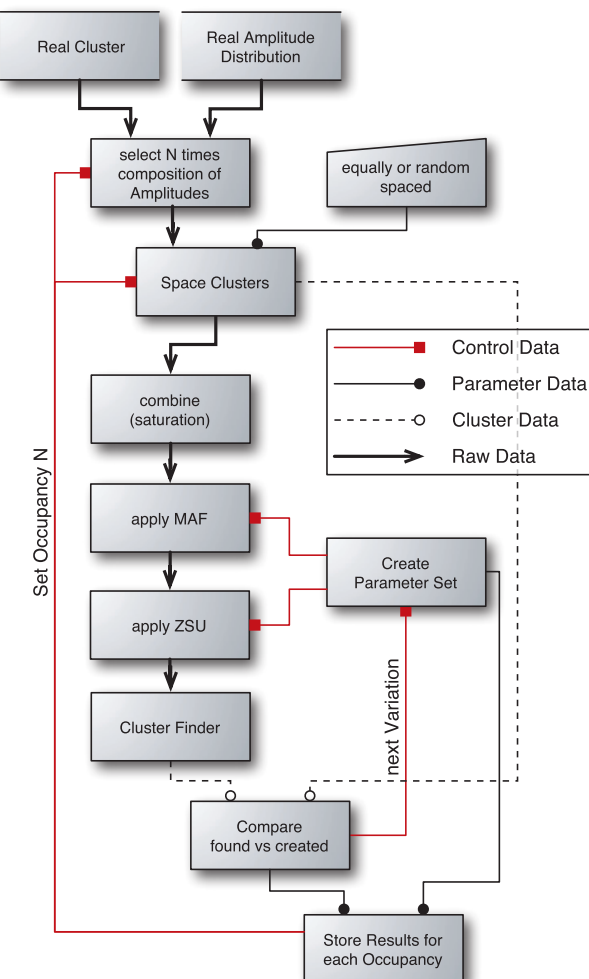
Zoom on the Shortening difference. Black is the original signal, green is the signal processed with the optimum set and red is the signal with the correlated set



Zoom on the Undershoot difference. Black is the original signal, green is the signal processed with the optimum set and red is the signal with the correlated set.

The parameter set of this two units is correlated, since the goal is to keep all signal information but also get a good compression. As described in the ALTRO chapter the ZSU removes all samples below a threshold. It can happen that due to pile up effects a small signal would fall below the ZSU threshold. This can be cured by the BSC2 unit, as long as the BSC2 can track the baseline. When allowing the BSC2 a large acceptance window it can happen that it will follow partially a signal and then never get track again of the real baseline. With the use of the pre and post samples this overreaction can be removed but the amount of baseline ADC values gets decreased so that again it can happen that the BSC2 loses track.

The ZSU can only work and keep all signals as considered if the BSC2 stays on track or the baseline variation of the channel is smaller than the threshold. Since clusters with a big charge have a visible, long living and significant tail as discussed in chapter \rightarrow Iontail even low occupancy events can have baseline distortions harming small signals. When moving to high occupancy channels the distortion increase, so the basic assumption is that the optimising goal is to keep all clusters but maximise the compression, without loosing cluster information.



Flowchart of the BSC2 & ZSU finder

The result of this optimisation gives a set of possible parameters for each occupancy tested. This scheme is not implemented but parts are existing, like the MAF and ZSU units as described in the following chapter.

Altro++

As clearly indicated the ALTRO parameters will be optimised by using the digital chain of the ALTRO. To reduce the overhead in complexity, price and speed when introducing real hardware in this process a ALTRO simulator was developed. The aim was to build up a software module which reproduces exactly the results of a real chip on the cost of speed or precision. This includes a bit precise fixed point implementation of the TCF not a more accurate version which is possible with a CPU. The ALTRO++ can be configured to turn on and off individual units of the digital chain as also as an inconsistency the clipping can be turned off, which is impossible in the ALTRO. This feature is extremely helpful when analysing data which is dropping below zero.

There is a limitation, the AUTOCAL circuit (->FEC) can't be implemented since in the stored data the data in between two events is not stored. The ZSU in the ALTRO++ at the moment only calculates the compression factor, not the ALTRO data format. This will be implemented. Not implemented is the MEB since this is not needed in software.

Computing

The final ALICE TPC consists of roughly 560000 channels, assuming the worst case that each channel needs a different configuration for the digital processor additionally to the pedestals, this puts the attention on the computing time to extract these parameters. The stability of the parameters will define the update rate to revise or recalculate the parameters. Also the pure data volume which has to be transferred to the detector electronics pre a start of run requires a clear scheme. Finally this configuration data has to be archived for the offline data reconstruction [n5,n6]. This leads to the questions: computing time, computing frequency, data volume, storage frequency, which will not be broken up completely before the ALICE physics program starts.

Pedestals

Starting with the pedestals as partially the simplest problem and partially a quite problematic one. The computing time is neglectable, since only a few hundred events have to be parsed to get the mean pedestal value. Additionally this computation is completely independent for each channel and extremely simple, so this task can already be done in the RCU or later in the LDCs of the DAQ or the HLT nodes. The data for the pedestal calculation does not need to be archived any time. The problem of the pedestals is more the pure data volume, since for all channels nearly 700 MByte is needed. So the distribution of the data

should be done in parallel. As already partially existing and implemented the two data paths, the DDL or the DCS are usable as described in chapter Prototype. The Data volume for each RCU is from 5 to 10 MB depending on the position on the TPC, since pedestal data could be highly compressed by an entropy coder [n8] like the Huffman coding [n13] this volume can be reduced by a factor of five. So as long as the data will not be sent from one source to the detector both data paths, the 200 MB/s DDL or the 10 MB/s DCS are sufficient. For archiving this data can be slowly collected and centrally stored.

The calculation and storage frequency will not be known before the complete ALICE Setup is completed detector wise as also cooling and electronics wise. The upper limit can be defined by the experience of NA49 [n7] of three pedestal runs per running day.

TCF

The determination of the TCF parameters are showing a completely different picture of problems. The previously described scheme consists of several computing steps with different computing prerequisite. The pulse finder has at the moment an inspection rate of roughly 26000 channels/s of 500 timebins on an Opteron 246 [n9] system using xfs [n10] as file system and gcc 3.3.4 [n11] as compiler. To extract the coefficients for one found pulse the same system needs 0.2 s. The running time of the correlator is increasing quadratically from 1.2s for 100 to 30s for 1000 correlations without storing the correlated pulses and from 14s for 100 to 21m for 1000 correlations when storing the correlated pulses. The best set finder needs 50s to find the best set. The most time (90%) is spent by reading the current implementation of the data set, so a speed up to below 20s is easily possible.

The first problem is the uncertainty if each ALTRO channel needs its own optimised TCF parameter set or each ALTRO reducing the needed effort by a factor 16 or bigger structures like TPC rows or patches reducing again the needed effort by a factor of 6 to 30 so 96 to 480 in total. There is not enough data of pulses with a high amplitude to answer the question if there are differences in the ALTRO channels or in the different ALTROs which are big enough that a channel wise TCF configuration is needed. Another question is the stability of the sets, which should be quite high, since only changes in the signal shape affect the TCF. The complete chain can run in parallel since no communication in between the different set finding blocks is needed, so the calculation time scales with the number of CPUs in a Cluster.

Assuming the worst case that every of the 557568 channels need their own configuration and that 1000 channels, fulfilling the pulse finder requirements, are needed to extract the optimum set. I assume that 1 million events should be sufficient to get enough statistics on each channel leading to an inspection time of 6000h for one CPU. The extraction of the coefficients would take 30000h for one CPU. With out the major speed up due to the re implementation this scheme would be completely impossible since the calculation time would be still half a year on an 2000 CPU cluster. The correlator needs 4500h without writing and

finally to find the best set 8000h are needed. In total this leads to a quite big amount of data and computing time.

Program	1 CPU			Cluster	
	On Set per	Chip	Row	Patch	2000 CPUs
		Chip	Row	Patch	
Pulse Finder	6000	375	38	2.4	3
Coefficient Maker	30000	1900	200	12	15
Correlator	4500	290	30	1.8	2.3
Best Set Finder	8000	490	49	3	4
Total	48500	3055	317	19.2	24.3

Running time in hours of the different steps to extract the TCF Parameters

configuration as also the broadcast mode, if so the configuration parameters will be automatically send by the RCU to all channels on one FEC as long the commands support a broadcast, otherwise it automatically creates the sequence for the individual channels. This sequences can be translated into the FeC2 language [n14] to use the DDL by the intermediate step to write out this sequences as FeC2 script. This is included in the FeC2Writer. For the configuration using the InterCom Layer [n15] no intermediate step is needed, since the function creating the code sequences is called by this layer and returns the command block which is then handled by the DIM client server system. Later also the communication via the DDL will be incorporated into the DIM system.

The data source for the InstructionBlockCoder is a binary file encapsulated into a class (ConfigIO). This can be easily extended to communicate with a database without any need of changing the other parts of the system. The actual partitioning of the data is derived from the transport granularity, so all configuration data from one RCU is collected in one file.

BSC2 & ZSU

To optimise this parameter set it is not expected that these parameters differ for each channel, since they are mostly dependent on the occupancy. The problem here arises when scanning the complete parameter space since there are eight parameters with 6.6 trillion possible combinations per occupancy. Fortunately many combinations can be excluded, since they are quite senseless.

Configuration

When all parameters are extracted they have to be stored and prepared for sending them to the FEE. For this purpose a set of classes were implemented. There are encapsulations for the different hardware components:

- » **ALTROCOMMANDCODER**
- » **RCUCOMMANDCODER**
- » **BOARDCONTROLLERCOMMANDCODER**

By the use of the component encapsulation classes all commands can be translated in their correct bit pattern for the hardware. The extracted parameters are set via the use of the matching commands. Additionally to the ALTRO digital chain parameters the BC needs configuration of the controlling thresholds. Also included in the classes are functions to read and parse the various parameters and error registers.

The layer above is parted in the different interface encapsulations.

- » **INSTRUCTIONBLOCKCODER**
- » **CONFIGIO**
- » **FEC2WRITER**

The RCU has a memory where command sequences can be stored. The coding of this command blocks is encapsulated in the InstructionBlockCoder. It supports both configuration modes of the FEE, the individual channel

Ion Tail Analysis

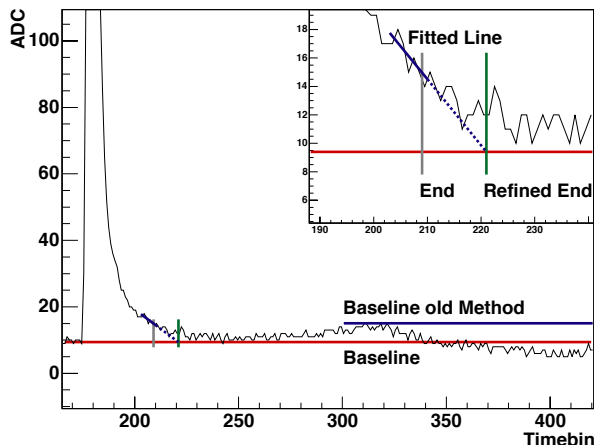
Ion Tail Analysis

During the analysis of the cosmic data of the test TPC an additional effect got visible following the normal signal tail. Since each avalanche signal is the result of the contribution of a large number of positive ions leaving the anode wire in various angles, so following different paths which can last for several tens of microseconds inducing a long ion tail as described in chapter (->TPC). At first the effect of the ion tail was visually found in cosmic data at the test TPC in pulses with extremely big amplitudes (>700 ADC) during the usage of the OM. After applying a moving average smoothing the shape of the ion tail was also found in clusters with smaller amplitudes (>200 ADC).

Neither the spread of the avalanche around the anode wire nor the variation from avalanche to avalanche has been accurately understood and quantified. Since this effect was visible in normal data a data based analysis was developed and due to the big influence of the gas mixture on the signal shape so also the ion tail the analysis was repeated for each gas mixture.

Pulse Extraction

To characterise the signal tail and its variation adequate pulses were extracted from the data. Like in the pulse finder of the TCF parameter extraction (page xx) single pulses of a minimum amplitude of 200 ADC at a early time position are needed since this fulfills the prerequisite of an complete, undisturbed and visible tail. The end of pulse position of the simple clusterfinder which is the time position of the last sample above the threshold of five is then refined for all remaining pulses. Since this method is insensitive on the tail shape but very sensitive to noise. The recalculation is based on a linear regression of a few samples around the previously calculated endpoint and the crossing point of the line with the baseline which then defines the new end point. This is shown in the plot below.

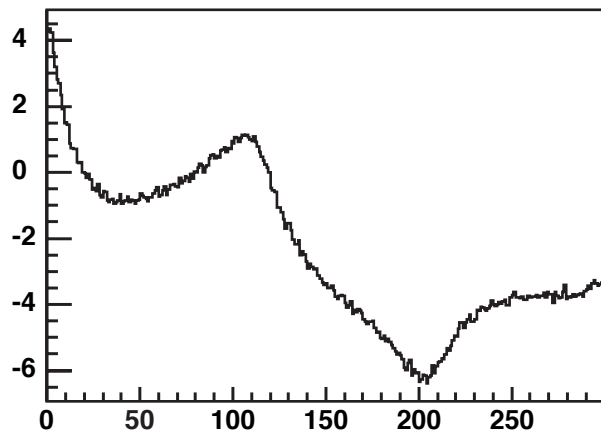


Part of extracted signal. The red line shows the new baseline calculation method, blue is the failing old one. In the zoomed view the linear regression around the pulsefinder end (6 pre, 2 post samples), the extrapolation and the refined end.

The endpoint of the pulses also defines the start point of the ion tail. From all pulses 500 timebins starting with the ion tail start point are then saved. This time window of 50 μ s (500 timebins with 10 MHz sampling frequency) The accuracy of the starting point of the ion tail is important since it is used to reshift all pulses to the same timing position.

It turned out that the cluster refinement is needed when using low clusterfinder thresholds, but the threshold used in the analysis threshold of ... kill CR

The determination of this point requires a proper knowledge of the baseline which is no problem during analysis of the cosmic data as described in (-> setup ?) since a proper baseline table and a correct mapping procedure exists. In the testbeam data this is not the case. As described in ->FeatureExtraction the extraction of a correct baseline table is possible with additional data reject and check algorithms but for the tail analysis the mapping of the AltroAddress of the baseline pattern or value to the correct AltroAddress in the data is problematic, since the address can be incorrect in the data. If applying the filter used by the baseline pattern extraction the statistics for sufficient pulses is dramatically reduced and renders a tail feature extraction at high maximum ADC values or high pulse charges impossible. Additionally the filter is not completely correct since switched address errors are not found, so wrongly reshifted ion tails would spoil the analysis which is quite sensitive to small errors due to the small signal itself. So the baseline for each pulse has to be extracted of the channel hosting the pulse. the first approach used the in ->Monitor described double threshold scheme which lead to a extreme signal drop as shown in the following plot, which was not discovered in different data.

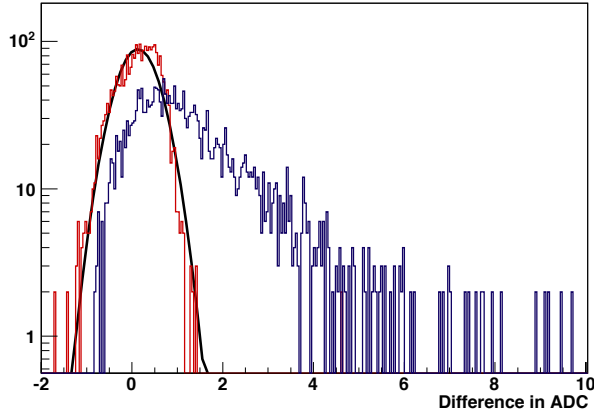


Mean of Ion Tail of all pulses of $600 < \text{max ADC} < 700$ using the old baseline calculation. The signal drops by 4 ADC.

This was caused by the limitation of the double threshold baseline calculation, which can fail following the tail if the mean of all samples lifts the thresholds away from the signal baseline, as shown in the plot to the left.

This method was replaced by a more precise and also stable one, which extracts an ADC histogram of all ADC values after the gating grid pulse of the channel and then calculates the mean of the channel by using the most probable

bin with a configurable amount of bins next to it. Since this analysis searches for a signal drop after the pulse an asymmetric window with only one lower bin and three higher bins was chosen to minimise the ion tail influence on the baseline calculation. To check the performance of this method the pedestal table and the wrong address filter was used. The remaining mapping failures were discarded by comparing the file baseline with the dynamic one. If the difference was bigger than two ADC the plot was displayed and checked via the eye. After removing the ambiguous addresses by the eye scan nearly no outliers of the new method are left as shown in the plot below, which also includes the double threshold calculation result.



Difference (dynamic - file) in between the file based baseline and the two dynamic baseline calculation methods. The red line is the new method, which is quite symmetric (mean = 0.13, σ = 0.46). The blue line is the double threshold scheme which clearly shows a trend to overestimate the baseline (mean = 1.7, RMS = 2.6).

This method works for all pulses in a low occupancy environment, which was a prerequisite of this analysis as long as there are no slow developing effects.

Additionally the ALTRO++ class (ref) is integrated here, to check the performance of the ALTRO digital circuit to remove disturbances like this ion tail.

All extracted signals are stored in a ROOT File as histograms. This are the time normalised tails as pure ADC values and as smoothed values by the moving average calculation as data. To check the analysis additional data is stored, this are complete pulses, histograms on all applied cuts and histograms to crosscheck the baseline calculation and validity of the cluster end refinement. Additionally all cut parameters and cluster informations are stored.

Cosmics

All pulses are separated in maximum ADC or pulse charge classes and the mean of this class is calculated.

The mean of each class is calculated. To extract the spread of the ion tail all pulses in their classes are overlaid in an hit plot.

Literaturverzeichniss

The Experiment

- [1] ALICE COLLABORATION; Homepage; <http://alice.web.cern.ch/Alice/AliceNew/>
- [2] ALICE COLLABORATION; »Technical Proposal«; CERN/LHCC/95-71, ISBN 92-9083-077-8; December 1995
- [3] ALICE COLLABORATION; »Technical Proposal Addendum 1«; CERN/LHCC/96-32
- [4] ALICE COLLABORATION; »Technical Proposal Addendum 2«; CERN/LHCC/99-13
- [5] ALICE COLLABORATION; »Physics Performance Report«; CERN/LHCC/2003-049, ISBN 92-9083-210-X; November 2003; <http://alice.web.cern.ch/Alice/ppr/web/PPRVICurrentVersion.html>
- [6] ALICE COLLABORATION; »TDR of the Dimuon Forward Spectrometer«; CERN/LHCC/99-22, ISBN 92-9083-148-0; August 1999; <https://edms.cern.ch/document/470838/>
- [7] ALICE COLLABORATION; »TDR of the Inner Tracking System«; CERN/LHCC/99-12, ISBN 92-9083-144-8; June 1999; <https://edms.cern.ch/document/398932/>
- [8] ALICE COLLABORATION; »TDR of the Time Projection Chamber«; CERN/LHCC/2000-001, ISBN 92-9083-155-3; January 2000; <https://edms.cern.ch/document/398930/>
- [9] ALICE COLLABORATION; »TDR of the Transition Radiation Detector«; CERN/LHCC/2001-021, ISBN 92-9083-184-7; October 2001; <https://edms.cern.ch/document/398057/>
- [10] ALICE COLLABORATION; »TDR of the Time of Flight System«; CERN/LHCC/2002-016, ISBN 92-9083-192-8; April 2002; <https://edms.cern.ch/document/460192/>
- [11] ALICE COLLABORATION; »TDR of the High Momentum Particle Identification Detector«; CERN/LHCC/98-19, ISBN 92-9083-134-0; August 1998; <https://edms.cern.ch/document/316545/>
- [12] ALICE COLLABORATION; »TDR of the Photon Spectrometer«; CERN/LHCC/99-4, ISBN 92-9083-138-3; March 1999; <https://edms.cern.ch/document/398934/>
- [13] ALICE COLLABORATION; Homepage of the Forward Multiplicity Detector; <http://fmd.nbi.dk/>
- [14] B. CHEYNIS, L. DUCROUX, E. GANGLER, J.Y. GROSSIORD, R. GUERNANE, A. GUICHARD; »For a V0 detector dedicated to the pp->2my+X physics in ALICE«; ALICE/INT-2000-29; November 2000; <https://edms.cern.ch/document/303914/>
- [15] ALICE COLLABORATION; Homepage of the T0 Detector; <http://fmd.nbi.dk/>
- [16] ALICE COLLABORATION; »TDR of the Photon Multiplicity Detector«; CERN/LHCC/99-32, ISBN 92-9083-153-7; September 1999; <https://edms.cern.ch/document/398931/>
- [17] ALICE COLLABORATION; »TDR of the Zero Degree Calorimeter«; CERN/LHCC/99-5, ISBN 92-9083-139-1; March 1999; <https://edms.cern.ch/document/398933/>
- [18] S. V. AFANASIEV ET AL. FOR THE NA49 COLLABORATION; »The NA49 large acceptance hadron detector«; Nucl. Instr. and Meth. A430, 210-244; 1999
- [19] M. ANDERSON ET AL. ; »The STAR Time Projection Chamber: A Unique Tool for Studying High Multiplicity Events at RHIC«; Nucl. Instrum. Meth. A 499, 659; 2003; http://www.star.bnl.gov/~jhthomas/NimWeb/tpc/tpc_nim.pdf
- [20] ALICE COLLABORATION; »TDR of the Trigger, Data Aquisition, High Level Trigger and Control System«; CERN/LHCC/1003-062, ISBN 92-9083-217-7 January 2004; <https://edms.cern.ch/document/456354/>
- [21] W. BLUM AND L. ROLANDI; »Particle Detection with Drift Chambers«; Springer Verlag, Berlin, Heidelberg, New York, ISBN 3-540-56425-X; 1993
- [22] H. A. BETHE; Annalen der Physik 5, p. 325; 1930
- [23] F. BLOCH; Z. Physik 81, p. 363; 1933
- [24] BETHE BLOCH AND I. LEHRHAUS ET AL.; IEEE Trans. Nucl. Sci. NS-30 p. 50; 1983
- [25] R VEENHOF; »Choosing a gas mixture for the ALICE TPC«; ALICE-INT-2003-29; May 2003; <https://edms.cern.ch/document/404406/>
- [26] CONSTI
- [27] A. PEISERT AND F. SAULI; »Drift and diffusion of electrons in gases«; CERN Report 84-08; 1984
- [28] L. G. H. HUXLEY AND R. W. CROMPTON; »The diffusion and drift of electrons in gases«; Wiley, New York; 1974
- [29] STEPHEN BIAGI; »Magboltz 2«; Nucl. Instr. and Meth. A421 234-240; 1999; <http://ref.web.cern.ch/ref/CERN/CNL/2000/001/Pr/magboltz>
- [30] F. SAULI; »Principles of Operation of Multiwire Proportional and Drift Chambers«; CERN Report 77-09, p. 79 – 183; 1977
- [31] B. MOTA; »Time-Domain Signal Processing Algorithms and their Implementation in the ALTRO chip for the ALICE TPC«; Ecole Polytechnique Fédérale de Lausanne; May 2003; <http://doc.cern.ch/archive/electronic/cernl/preprints/thesis/thesis-2003-023.pdf>
- [32] S. MARIDOR; »L3 Magnet - ALICE Experiment«; https://edms.cern.ch/cdd/plsql/c4w_edms_logon?jump=SEARCH&p1=DIRECT&p2=ALI3DDET0001&p3=AB
- [33] R. BRAMM; »TPC-Test Data Page«; <http://pcikf49.ikf.physik.uni-frankfurt.de/-tpc/> or via <http://www.ikf.physik.uni-frankfurt.de/-alice/>

Front End Electronic

[n1] L. MUSA*, J. BAECHLER, N. BIALAS, R. BRAMM, R. CAMPAGNOLO, C. ENGSTER, F. FORMENTI, U. BONNES, R. ESTEVE BOSCH, U. FRANKENFELD, P. GLASSEL, C. GONZALEZ, H.-A. GUSTAFSSON, A. JIMÉNEZ, A. JUNIQUE, J. LIEN, V. LINDENSTRUTH, B. MOTA, P. BRAUN-MUNZINGER, H. OESCHLER, L. OSTERMAN, R. RENFORDT, G. RÜSCHMANN, D. RÖHRICH, H.-R. SCHMIDT, J. STACHEL, A.-K. SOLTVEIT, K. ULLALAND; »The ALICE TPC Front End Electronics«; Proceedings of the IEEE Nuclear Science Symposium, Portland; 20 - 25 Oct 2003; <http://ep-ed-alice-tpc.web.cern.ch/ep-ed-alice-tpc/doc/papers/INSS2003.pdf>

[n2] ST MICROELECTRONICS; »Datasheet of the TSA1001 A/D Converter«; 2004; <http://www.st.com/stonline/books/pdf/docs/7333.pdf>

[n3] L. DUGOUJON, S. ENGELS, R. ESTEVE-BOSCH, B. MOTA, L. MUSA, A. JIMÉNEZ-DE-PARGA, D. SUBIELA; »A Low-Power 16-channel AD Converter and Digital Processor ASIC«; Proc. of the ESSCIRC, Florence, Italy; September 2002; <http://ep-ed-alice-tpc.web.cern.ch/ep-ed-alice-tpc/doc/papers/ESSCERC2002.pdf>

[n4] R. ESTEVE BOSCH, A. JIMÉNEZ DE PARGA, B. MOTA, AND L. MUSA; »The ALTRO Chip: A 16-Channel A/D Converter and Digital Processor for Gas Detectors«; IEEE Transaction on Nuclear Science, Vol. 50 No. 6; December 2003; http://ep-ed-alice-tpc.web.cern.ch/ep-ed-alice-tpc/doc/papers/TNS_alth_Dic2003.pdf

[n5] L. MUSA ET AL. ; »ALICE TPC Readout Chip Users Manual«; CERN EP/ED; June 2002; http://ep-ed-alice-tpc.web.cern.ch/ep-ed-alice-tpc/doc/ALTRO_CHIP/UserManual_draft_02.pdf

[n6] ALICE COLLABORATION; »TDR of the Time Projection Chamber«; CERN/LHCC/2000-001, ISBN 92-9083-155-3; January 2000; <https://edms.cern.ch/document/398930/1>

[n7] B. MOTA ET AL.; »Digital Implementation of a Tail Cancellation Filter for the Time Projection Chamber of the ALICE Experiment.«; Proc of the 6 Workshop on Electronics for LHC Experiments, Krakow; September, 11-15, 2000; <http://ep-ed-alice-tpc.web.cern.ch/ep-ed-alice-tpc/doc/papers/filter.pdf>

[n8] B. MOTA; »Time-Domain Signal Processing Algorithms and their Implementation in the ALTRO chip for the ALICE TPC«; Ecole Polytechnique Fédérale de Lausanne; May 2003; <http://doc.cern.ch/archive/electronic/cern/preprints/thesis/thesis-2003-023.pdf>

[n9] ALICE TPC FRONT END ELECTRONICS; Homepage; <http://ep-ed-alice-tpc.web.cern.ch/ep-ed-alice-tpc/>

[n10] J. A. LIEN ET AL.; »Readout Control Unit of the Front end Electronics for the ALICE Time Projection Chamber«; Proceedings of the 8th Workshop on Electronics for LHC Experiments, Colmar, France; 9-13 September 2002 <http://doc.cern.ch/archive/cernrep/2002/2002-003/p160.pdf>

[n11] ARM LIMITED; »ARM T922 Core Data Sheet«; <http://www.arm.com/products/CPUs/ARM922T.html>

[n12] µCLINUX; »µLinux Embedded Linux/Microcontroller Project«; <http://www.uclinux.org/>

[n13] PASA; Homepage; <http://ep-ed-alice-tpc.web.cern.ch/ep-ed-alice-tpc/pasa.htm>

[n14] ALTRO Bus, BACKPLANE; Homepage; http://ep-ed-alice-tpc.web.cern.ch/ep-ed-alice-tpc/altro_bus.htm

[n15] RCU; Homepage; <http://ep-ed-alice-tpc.web.cern.ch/ep-ed-alice-tpc/rcu1.htm> & <http://www.fi.uib.no/~pommer/rcu/>

[n16] ALICE COLLABORATION; »TDR of the Trigger, Data Aquisition, High Level Trigger and Control System«; CERN/LHCC/1003-062, ISBN 92-9083-217-7 January 2004; <https://edms.cern.ch/document/456354/1>

[n17] P. W. NICHOLSON; »Nuclear Electronics«; Wiley Interscience, ISBN 0-471-63687-5; 1969

[n18] C. H. NOWLIN AND J. L. BLANKENSHIP; Rev.Sci. Instr. 36, p. 599-605; 1965

Jitter

Prototype Environment

[n1] PLDAPPLICATIONS; »Standard Prototyping PCI Boards«; http://www.plda.com/pdt_boards_pci.htm

[n2] PLDAPPLICATIONS; »Interlectual Property Cores«; http://www.plda.com/pdt_core_pci.htm

[n3] B. W. KERNIGHAN AND D. M. RITCHIE; Whitepaper: »The C Programming Language«; Prentice-Hall: Englewood Cliffs, NJ, 1978. Second edition, 1988

[n4] NATIONAL INSTRUMENTS; »LabVIEW«; <http://www.ni.com/labview/>

[n5] RENE BRUN, FONS RADEMAKERS; »ROOT an object orientated Data Analysis Framework«; root.cern.ch

[n6] Bjarne STRUSTRUP; Whitepaper: »The C++ Programming Language«; Addison Wesley, 1985. Second edition, 1991, Third Edition 1997, ISBN 02-0188-9544

[n7] MASAHIRO GOTO; »CINT a C/C++ interpreter«; <http://root.cern.ch/root/Cint.html>

[n8] OPENGL; »The Industry's Foundation for High Performance Graphics«; <http://www.opengl.org/>

[n9] E. DÉNES; »Instructions for FeC2 (Front-End Control and Configuration) program«; http://alice-proj-dll.web.cern.ch/alice-proj-dll/doc/FeC2_syntax.txt

- [n10] C. KOFLER, S. BABLOK; »Alice-FEEControl«; <http://www.ztt.fb-worms.de/en/projects/Alice-FEEControl/index.shtml>
- [n11] ALICE DATE GROUP; »ALICE DATE V4 User's Guide«; ALICE/INT-2002-036 v.1; November 2002; <https://edms.cern.ch/document/362104/1>
- [n12] R. DIVIÀ; »DATE header reference card«; <http://aldwww.cern.ch/>
- [n13] L. MUSA; »TPC Data Format for the may 2004 in-Beam Test«; <http://ep-ed-alice-tpc.web.cern.ch/ep-ed-alice-tpc/>
- [n14] L. MUSA ET AL. ; »ALICE TPC Readout Chip Users Manual«; CERN EP/ED; June 2002; http://ep-ed-alice-tpc.web.cern.ch/ep-ed-alice-tpc/doc/ALTRO_CHIP/UserManual_draft_02.pdf
- [n15] ALICE COLLABORATION; »TDR of the Trigger, Data Aquisition, High Level Trigger and Control System«; CERN/LHCC/1003-062, ISBN 92-9083-217-7 January 2004; <https://edms.cern.ch/document/456354/1>
- [n16] R. BRAMM ET AL.; »High-level trigger system for the LHC ALICE experiment«; Nucl. Instrum. Methods Phys. Res., A 502 p. 441-442; 2003; [http://dx.doi.org/10.1016/S0168-9002\(03\)00463-7](http://dx.doi.org/10.1016/S0168-9002(03)00463-7)
- [n17] T. STEINBECK; »A Modular and Fault-Tolerant Data Transport Framework«; arXiv:cs.DC/0404014v1; April 2004; <http://de.arxiv.org/pdf/cs.DC/0404014>
- [n18] ALICE TPC GROUP; »ROC and Pad Numbering Convention«
- [n19] RENE BRUN, FONS RADEMAKERS; »ROOT porting status«; <http://root.cern.ch/root/Porting.html>
- [n20] LINUX; »The Linux Kernel«; <http://www.kernel.org/>
- [n21] R. BRAMM; »TPC-Test Data Page«; <http://pcikf49.ikf.physik.uni-frankfurt.de/~tpc1/ or via http://www.ikf.physik.uni-frankfurt.de/~alice/>
- [n22] CASTOR; »CASTOR«; <http://castor.web.cern.ch/castor/>
- [n23] J. P. BAUD, B. COUTURIER, C. CURRAN, J. D. DURAND, E. KNEZO, S. OCCHETTI, O. BÄRRING; »CASTOR status and evolution«; Conference for Computing in High-Energy and Nuclear Physics, cs.OH/0305047;2003; <http://arxiv.org/abs/cs.OH/0305047>
- [n5] ALICE COLLABORATION; »Physics Performance Report«; CERN/LHCC/2003-049, ISBN 92-9083-210-X; November 2003; <http://alice.web.cern.ch/Alice/ppr/web/PPRVICurrentVersion.html>
- [n6] ALICE OFF-LINE PROJECT; Homepage; <http://aliweb.cern.ch/offline/>
- [n7] S. V. AFANASIEV ET AL. FOR THE NA49 COLLABORATION; »The NA49 large acceptance hadron detector«; Nucl. Instr. and Meth. A430, 210-244; 1999
- [n8] C. E. SHANNON; »Mathematical theory of communication«; Bell System Technical Journal, 27:379-423; 1948
- [n9] AMD; »Opteron Processor«; http://www.amd.com/us-en/Processors/ProductInformation/0,,30_118_8825,00.html
- [n10] SGI; »XFS A high-performance journaling filesystem«; <http://oss.sgi.com/projects/xfs/>
- [n11] GNU; »gcc Homepage«; <http://gcc.gnu.org/>
- [n12] L. MUSA ET AL. ; »ALICE TPC Readout Chip Users Manual«; CERN EP/ED; June 2002; http://ep-ed-alice-tpc.web.cern.ch/ep-ed-alice-tpc/doc/ALTRO_CHIP/UserManual_draft_02.pdf
- [n13] D. A. HUFFMAN; »A method for the construction of minimum redundancy codes«; In Proc. IRE 40, volume 10, pages 1098–1101; September 1952
- [n14] E. DÉNES; »Instructions for FeC2 (Front-End Control and Configuration) program«; http://alice-proj-dll.web.cern.ch/alice-proj-dll/doc/FeC2_syntax.txt
- [n15] C. KOFLER, S. BABLOK; »Alice-FEEControl«; <http://www.ztt.fb-worms.de/en/projects/Alice-FEEControl/index.shtml>

ALTRO Parameter Optimising

- [n1] ALICE TPC FRONT END ELECTRONICS; Homepage; <http://ep-ed-alice-tpc.web.cern.ch/ep-ed-alice-tpc/>
- [n2] B. MOTA; »Time-Domain Signal Processing Algorithms and their Implementation in the ALTRO chip for the ALICE TPC«; Ecole Polytechnique Fédérale de Lausanne; May 2003; <http://doc.cern.ch/archive/electronic/cern/preprints/thesis/thesis-2003-023.pdf>
- [n3] THE MATHWORKS, INC.; »MATLAB«; <http://www.mathworks.com/products/matlab/>
- [n4] R. BRAMM; »TPC-Test Data Page«; <http://pcikf49.ikf.physik.uni-frankfurt.de/~tpc1/ or via http://www.ikf.physik.uni-frankfurt.de/~alice/>

Pulse Finder

pulseFinder, extracts selected pulses and denoises the tail.

Run Parameters :

- t, --EventType :
sets the eventtype: [mandatory]
DATEFile = Testbeam DATE events
- rn, --Runnumber :
sets the runnumber [mandatory]
- rp, --RunPath :
sets path to the run [mandatory]
- n, --EventCount :
number of events [default: 1000]
- o, --OutPlace :
Path to the Output dir for the results [mandatory]
BAWARE Folder MUST exist

Pulse Finder Parameters:

- pa, --PreAquisitionSamples :
Pre Aquisition Samples. [default: 40]
- ps --PreSamples :
Number of Presamples where no signal is allowed, to circumvent Pulses before event start. [default: 5]
- pt --PreSampleThreshold :
Threshold to define what is a pulse in the presample area [default: 20]
- ah --MaxADCThreshold :
Max ADCThreshold, upper boundarys to specify which clusters are to be found [mandatory]
- al --MinADCThreshold :
Min ADCThreshold, lower boundarys to specify which clusters are to be found [mandatory]
- sp --MaxTimePosition :
Maximum Time Position of Pulse [mandatory]
BEWARE ! The programm always assumes 1024 timebins max !
- ct --PulseThreshold :
Threshold, from where on somthing is called a pulse [default: 10]
- cs --NeededSuccessiveADC :
Number of consecutive Samples above PulseThreshold needed to define a Pulse [default: 3]
- cf --FitThreshold :
Factor to specify level of end of cluster. means maxadc*FitThreshold [default: 0.1]
- ia --IntegralVSampThreshold :
Integral vs Amplitude Threshold, to filter out double clusters [default: 4.5]

Moving Average Parameters/Smoothing parameters:

- ml --MALeftSamples :
MALeftSamples samples left to actual Point [default: 3]
- mr --MARightSamples :
MARightSamples samples right to actual Point [default: 4]
- md --MADirection :
Direction > 0 = from left to right; < 0 = vice versa [default: 1]
- gt --AllowedGlitchesinSignal :
Allowed Glitches in Signal threeshold [default: 5]

General Parameters:

- d --DebugLevel :
Sets the debuglevel [default: 0]
- h --help :
Shows help, exactly what you see now
- v --version :
Show revision

example: ./pulseFinder.app -t DATEfile -rn 820 -rp /Volumes/Daten/TestBeam/ -o ./teststart/ -n 1000 -d 0 -ah 900 -al 500 -sp 200

Pedestal Calculation log

0 Event: 14 secondEquipment: 0 DefChannels: 1552 double Addresses: 1552 = 100 overflow Addresses: 0 = 0 Invalid Addresses: 0 = 0

1 Event: 47 secondEquipment: 0 DefChannels: 4 double Addresses: 4 = 100 overflow Addresses: 0 = 0 Invalid Addresses: 0 = 0

2 Event: 66 secondEquipment: 0 DefChannels: 4 double Addresses: 4 = 100 overflow Addresses: 0 = 0 Invalid Addresses: 0 = 0

3 Event: 77 secondEquipment: 0 DefChannels: 2714 double Addresses: 2714 = 100 overflow Addresses: 0 = 0 Invalid Addresses: 0 = 0

4 Event: 79 secondEquipment: 0 DefChannels: 2418 double Addresses: 2418 = 100 overflow Addresses: 0 = 0 Invalid Addresses: 0 = 0

5 Event: 101 secondEquipment: 0 DefChannels: 1800 double Addresses: 1800 = 100 overflow Addresses: 0 = 0 Invalid Addresses: 0 = 0

6 Event: 109 secondEquipment: 0 DefChannels: 1144 double Addresses: 1144 = 100 overflow Addresses: 0 = 0 Invalid Addresses: 0 = 0

7 Event: 136 secondEquipment: 0 DefChannels: 4 double Addresses: 4 = 100 overflow Addresses: 0 = 0 Invalid Addresses: 0 = 0

8 Event: 141 secondEquipment: 0 DefChannels: 2 double Addresses: 2 = 100 overflow Addresses: 0 = 0 Invalid Addresses: 0 = 0

9 Event: 171 secondEquipment: 0 DefChannels: 4 double Addresses: 4 = 100 overflow Addresses: 0 = 0 Invalid Addresses: 0 = 0

10 Event: 178 secondEquipment: 0 DefChannels: 790 double Addresses: 790 = 100 overflow Addresses: 0 = 0 Invalid Addresses: 0 = 0

11 Event: 186 secondEquipment: 0 DefChannels: 3018 double Addresses: 3018 = 100 overflow Addresses: 0 = 0 Invalid Addresses: 0 = 0

12 Event: 188 secondEquipment: 0 DefChannels: 2268 double Addresses: 2268 = 100 overflow Addresses: 0 = 0 Invalid Addresses: 0 = 0

13 Event: 189 secondEquipment: 0 DefChannels: 3154 double Addresses: 3072 = 97 overflow Addresses: 0 = 0 Invalid Addresses: 82 = 2

14 Event: 190 secondEquipment: 0 DefChannels: 582 double Addresses: 582 = 100 overflow Addresses: 0 = 0 Invalid Addresses: 0 = 0

15 Event: 197 secondEquipment: 0 DefChannels: 1624 double Addresses: 1624 = 100 overflow Addresses: 0 = 0 Invalid Addresses: 0 = 0

16 Event: 206 secondEquipment: 0 DefChannels: 2 double Addresses: 2 = 100 overflow Addresses: 0 = 0 Invalid Addresses: 0 = 0

17 Event: 229 secondEquipment: 0 DefChannels: 4 double Addresses: 4 = 100 overflow Addresses: 0 = 0 Invalid Addresses: 0 = 0

18 Event: 235 secondEquipment: 0 DefChannels: 4 double Addresses: 4 = 100 overflow Addresses: 0 = 0 Invalid Addresses: 0 = 0

19 Event: 236 secondEquipment: 0 DefChannels: 2158 double Addresses: 2158 = 100 overflow Addresses: 0 = 0 Invalid Addresses: 0 = 0

20 Event: 239 secondEquipment: 0 DefChannels: 2 double Addresses: 2 = 100 overflow Addresses: 0 = 0 Invalid Addresses: 0 = 0

21 Event: 251 secondEquipment: 0 DefChannels: 2588 double Addresses: 2588 = 100 overflow Addresses: 0 = 0 Invalid Addresses: 0 = 0

22 Event: 269 secondEquipment: 0 DefChannels: 2 double Addresses: 2 = 100 overflow Addresses: 0 = 0 Invalid Addresses: 0 = 0

23 Event: 310 secondEquipment: 0 DefChannels: 4 double Addresses: 4 = 100 overflow Addresses: 0 = 0 Invalid Addresses: 0 = 0

24 Event: 314 secondEquipment: 0 DefChannels: 2056 double Addresses: 2056 = 100 overflow Addresses: 0 = 0 Invalid Addresses: 0 = 0

25 Event: 335 secondEquipment: 0 DefChannels: 1730 double Addresses: 1730 = 100 overflow Addresses: 0 = 0 Invalid Addresses: 0 = 0

26 Event: 339 secondEquipment: 0 DefChannels: 1432 double Addresses: 1432 = 100 overflow Addresses: 0 = 0 Invalid Addresses: 0 = 0

27 Event: 359 secondEquipment: 0 DefChannels: 2038 double Addresses: 2038 = 100 overflow Addresses: 0 = 0 Invalid Addresses: 0 = 0

28 Event: 361 secondEquipment: 0 DefChannels: 3008 double Addresses: 3008 = 100 overflow Addresses: 0 = 0 Invalid Addresses: 0 = 0

29 Event: 384 secondEquipment: 0 DefChannels: 2744 double Addresses: 2744 = 100 overflow Addresses: 0 = 0 Invalid Addresses: 0 = 0

30 Event: 396 secondEquipment: 0 DefChannels: 2 double Addresses: 2 = 100 overflow Addresses: 0 = 0 Invalid Addresses: 0 = 0

31 Event: 400 secondEquipment: 0 DefChannels: 1814 double Addresses: 1814 = 100 overflow Addresses: 0 = 0 Invalid Addresses: 0 = 0

32 Event: 404 secondEquipment: 0 DefChannels: 2908 double Addresses: 2908 = 100 overflow Addresses: 0 = 0 Invalid Addresses: 0 = 0

33 Event: 407 secondEquipment: 0 DefChannels: 1792 double Addresses: 1792 = 100 overflow Addresses: 0 = 0 Invalid Addresses: 0 = 0

34 Event: 424 secondEquipment: 0 DefChannels: 924 double Addresses: 924 = 100 overflow Addresses: 0 = 0 Invalid Addresses: 0 = 0

35 Event: 432 secondEquipment: 0 DefChannels: 1748 double Addresses: 1748 = 100 overflow Addresses: 0 = 0 Invalid Addresses: 0 = 0

36 Event: 433 secondEquipment: 0 DefChannels: 1052 double Addresses: 1052 = 100 overflow Addresses: 0 = 0 Invalid Addresses: 0 = 0

37 Event: 478 secondEquipment: 0 DefChannels: 3132 double Addresses: 3072 = 98 overflow Addresses: 0 = 0 Invalid Addresses: 60 = 1

38 Event: 492 secondEquipment: 0 DefChannels: 2574 double Addresses: 2574 = 100 overflow Addresses: 0 = 0 Invalid Addresses: 0 = 0

39 Event: 522 secondEquipment: 0 DefChannels: 1794 double Addresses: 1794 = 100 overflow Addresses: 0 = 0 Invalid Addresses: 0 = 0

40 Event: 531 secondEquipment: 0 DefChannels: 4 double Addresses: 4 = 100 overflow Addresses: 0 = 0 Invalid Addresses: 0 = 0

41 Event: 533 secondEquipment: 0 DefChannels: 4 double Addresses: 4 = 100 overflow Addresses: 0 = 0 Invalid Addresses: 0 = 0

42 Event: 578 secondEquipment: 0 DefChannels: 1350 double Addresses: 1350 = 100 overflow Addresses: 0 = 0 Invalid Addresses: 0 = 0

43 Event: 580 secondEquipment: 0 DefChannels: 1596 double

```

Addresses: 1596 = 100 overflow Addresses: 0 = 0 Invalid
Addresses: 0 = 0
44 Event: 609 secondEquipment: 0 DefChannels: 3117 double
Addresses: 3072 = 98 overflow Addresses: 0 = 0 Invalid
Addresses: 45 = 1
45 Event: 619 secondEquipment: 0 DefChannels: 1844 double
Addresses: 1844 = 100 overflow Addresses: 0 = 0 Invalid
Addresses: 0 = 0
46 Event: 620 secondEquipment: 0 DefChannels: 166 double
Addresses: 166 = 100 overflow Addresses: 0 = 0 Invalid
Addresses: 0 = 0
47 Event: 637 secondEquipment: 0 DefChannels: 3113 double
Addresses: 3072 = 98 overflow Addresses: 0 = 0 Invalid
Addresses: 41 = 1
48 Event: 650 secondEquipment: 0 DefChannels: 1832 double
Addresses: 1832 = 100 overflow Addresses: 0 = 0 Invalid
Addresses: 0 = 0
49 Event: 666 secondEquipment: 0 DefChannels: 4 double
Addresses: 4 = 100 overflow Addresses: 0 = 0 Invalid
Addresses: 0 = 0
50 Event: 677 secondEquipment: 0 DefChannels: 2132 double
Addresses: 2132 = 100 overflow Addresses: 0 = 0 Invalid
Addresses: 0 = 0
51 Event: 692 secondEquipment: 0 DefChannels: 2472 double
Addresses: 2472 = 100 overflow Addresses: 0 = 0 Invalid
Addresses: 0 = 0
52 Event: 695 secondEquipment: 0 DefChannels: 2458 double
Addresses: 2458 = 100 overflow Addresses: 0 = 0 Invalid
Addresses: 0 = 0
53 Event: 696 secondEquipment: 0 DefChannels: 1760 double
Addresses: 1760 = 100 overflow Addresses: 0 = 0 Invalid
Addresses: 0 = 0
54 Event: 701 secondEquipment: 0 DefChannels: 2 double
Addresses: 2 = 100 overflow Addresses: 0 = 0 Invalid
Addresses: 0 = 0
55 Event: 703 secondEquipment: 0 DefChannels: 2 double
Addresses: 2 = 100 overflow Addresses: 0 = 0 Invalid
Addresses: 0 = 0
56 Event: 706 secondEquipment: 0 DefChannels: 3296 double
Addresses: 3296 = 100 overflow Addresses: 0 = 0 Invalid
Addresses: 0 = 0
57 Event: 714 secondEquipment: 0 DefChannels: 4 double
Addresses: 4 = 100 overflow Addresses: 0 = 0 Invalid
Addresses: 0 = 0
58 Event: 718 secondEquipment: 0 DefChannels: 988 double
Addresses: 988 = 100 overflow Addresses: 0 = 0 Invalid
Addresses: 0 = 0
59 Event: 722 secondEquipment: 0 DefChannels: 1292 double
Addresses: 1292 = 100 overflow Addresses: 0 = 0 Invalid
Addresses: 0 = 0
60 Event: 778 secondEquipment: 0 DefChannels: 4338 double
Addresses: 4338 = 100 overflow Addresses: 0 = 0 Invalid
Addresses: 0 = 0
61 Event: 779 secondEquipment: 0 DefChannels: 2 double
Addresses: 2 = 100 overflow Addresses: 0 = 0 Invalid
Addresses: 0 = 0
62 Event: 790 secondEquipment: 0 DefChannels: 4 double
Addresses: 4 = 100 overflow Addresses: 0 = 0 Invalid
Addresses: 0 = 0
63 Event: 796 secondEquipment: 0 DefChannels: 4 double
Addresses: 4 = 100 overflow Addresses: 0 = 0 Invalid
Addresses: 0 = 0
64 Event: 813 secondEquipment: 0 DefChannels: 1834 double
Addresses: 1834 = 100 overflow Addresses: 0 = 0 Invalid
Addresses: 0 = 0
65 Event: 826 secondEquipment: 0 DefChannels: 1496 double
Addresses: 1496 = 100 overflow Addresses: 0 = 0 Invalid
Addresses: 0 = 0
66 Event: 885 secondEquipment: 0 DefChannels: 1504 double
Addresses: 1504 = 100 overflow Addresses: 0 = 0 Invalid
Addresses: 0 = 0
67 Event: 889 secondEquipment: 0 DefChannels: 726 double
Addresses: 726 = 100 overflow Addresses: 0 = 0 Invalid
Addresses: 0 = 0
68 Event: 890 secondEquipment: 0 DefChannels: 940 double
Addresses: 940 = 100 overflow Addresses: 0 = 0 Invalid
Addresses: 0 = 0
69 Event: 910 secondEquipment: 0 DefChannels: 2 double
Addresses: 2 = 100 overflow Addresses: 0 = 0 Invalid
Addresses: 0 = 0
70 Event: 914 secondEquipment: 0 DefChannels: 1936 double
Addresses: 1936 = 100 overflow Addresses: 0 = 0 Invalid
Addresses: 0 = 0
71 Event: 989 secondEquipment: 0 DefChannels: 2642 double
Addresses: 2642 = 100 overflow Addresses: 0 = 0 Invalid
Addresses: 0 = 0
72 Event: 991 secondEquipment: 0 DefChannels: 4 double
Addresses: 4 = 100 overflow Addresses: 0 = 0 Invalid
Addresses: 0 = 0
73 Event: 994 secondEquipment: 0 DefChannels: 4 double
Addresses: 4 = 100 overflow Addresses: 0 = 0 Invalid
Addresses: 0 = 0
-----
Channel : 3229 Timebin: 44 always excluded!! val: 0
Channel : 3229 Timebin: 49 always excluded!! val: 0
Channel : 3229 Timebin: 51 always excluded!! val: 0
Channel : 3229 Timebin: 53 always excluded!! val: 0
Channel : 3230 Timebin: 42 always excluded!! val: 0
Channel : 3230 Timebin: 44 always excluded!! val: 0
Channel : 3230 Timebin: 49 always excluded!! val: 0
Channel : 3230 Timebin: 51 always excluded!! val: 0
Channel : 3230 Timebin: 53 always excluded!! val: 0
Channel : 3231 Timebin: 42 always excluded!! val: 0
Channel : 3231 Timebin: 44 always excluded!! val: 0
Channel : 3231 Timebin: 49 always excluded!! val: 0
Channel : 3231 Timebin: 51 always excluded!! val: 0
Channel : 3231 Timebin: 53 always excluded!! val: 0
Channel : 3231 Timebin: 58 always excluded!! val: 0
Channel : 3231 Timebin: 60 always excluded!! val: 0
Channel : 3232 Timebin: 41 always excluded!! val: 0
Channel : 3232 Timebin: 43 always excluded!! val: 0
Channel : 3232 Timebin: 45 always excluded!! val: 0
Channel : 3232 Timebin: 49 always excluded!! val: 0
Channel : 3232 Timebin: 51 always excluded!! val: 0
Channel : 3232 Timebin: 53 always excluded!! val: 0
Channel : 3233 Timebin: 43 always excluded!! val: 0
Channel : 3233 Timebin: 45 always excluded!! val: 0
Channel : 3233 Timebin: 49 always excluded!! val: 0
Channel : 3233 Timebin: 51 always excluded!! val: 0
Channel : 3234 Timebin: 41 always excluded!! val: 0
Channel : 3234 Timebin: 43 always excluded!! val: 0
Channel : 3234 Timebin: 45 always excluded!! val: 0
Channel : 3234 Timebin: 49 always excluded!! val: 0
Channel : 3234 Timebin: 51 always excluded!! val: 0
Channel : 3234 Timebin: 53 always excluded!! val: 0
Channel : 3234 Timebin: 58 always excluded!! val: 0
Channel : 3234 Timebin: 60 always excluded!! val: 0
Channel : 3235 Timebin: 59 always excluded!! val: 0
Channel : 3236 Timebin: 63 always excluded!! val: 0
Channel : 3236 Timebin: 67 always excluded!! val: 0
Channel : 3237 Timebin: 163 always excluded!! val: 0
Channel : 3237 Timebin: 163 always excluded!! val: 0
Channel : 3237 Timebin: 181 always excluded!! val: 0
Channel : 3237 Timebin: 345 always excluded!! val: 0
Channel : 3237 Timebin: 363 always excluded!! val: 0
Channel : 3237 Timebin: 163 always excluded!! val: 0
Channel : 3237 Timebin: 183 always excluded!! val: 0
Channel : 3237 Timebin: 254 always excluded!! val: 0
Channel : 3237 Timebin: 272 always excluded!! val: 0
Channel : 3237 Timebin: 345 always excluded!! val: 0
Channel : 3237 Timebin: 363 always excluded!! val: 0
Channel : 3237 Timebin: 436 always excluded!! val: 0
Channel : 3237 Timebin: 145 always excluded!! val: 0
Channel : 3237 Timebin: 163 always excluded!! val: 0
Channel : 3237 Timebin: 181 always excluded!! val: 0
Channel : 3237 Timebin: 254 always excluded!! val: 0
Channel : 3237 Timebin: 272 always excluded!! val: 0
Channel : 3237 Timebin: 345 always excluded!! val: 0
Channel : 3237 Timebin: 363 always excluded!! val: 0
Channel : 3237 Timebin: 405 always excluded!! val: 0
Channel : 3237 Timebin: 436 always excluded!! val: 0
Channel : 3237 Timebin: 454 always excluded!! val: 0
Channel : 3237 Timebin: 90 always excluded!! val: 0
Channel : 3237 Timebin: 96 always excluded!! val: 0
Channel : 3237 Timebin: 114 always excluded!! val: 0
Channel : 3237 Timebin: 132 always excluded!! val: 0
Channel : 3237 Timebin: 145 always excluded!! val: 0
Channel : 3237 Timebin: 163 always excluded!! val: 0
Channel : 3237 Timebin: 181 always excluded!! val: 0
Channel : 3237 Timebin: 236 always excluded!! val: 0
Channel : 3237 Timebin: 254 always excluded!! val: 0
Channel : 3237 Timebin: 272 always excluded!! val: 0
Channel : 3237 Timebin: 327 always excluded!! val: 0
Channel : 3237 Timebin: 345 always excluded!! val: 0
Channel : 3237 Timebin: 405 always excluded!! val: 0
Channel : 3237 Timebin: 418 always excluded!! val: 0
Channel : 3237 Timebin: 436 always excluded!! val: 0
Channel : 3237 Timebin: 454 always excluded!! val: 0
Channel : 3237 Timebin: 460 always excluded!! val: 0
Channel : 3407 Timebin: 163 always excluded!! val: 0
-----
-----  

Count 'DefChannels: 2' : 9  

Count 'DefChannels > 2' : 65  

Count 'overflow Addresses > 0' : 0  

Count 'Invalid Addresses > 0' : 4  

Total Errors : 74 = 7%  

Total Events : 1000 Events Analysed.

```

make coefficients

```

[pcikf49:AliceTPC/AltroOptimisation/trunk] rbramm% ./  

makeCoefficients.app -h  

writePulsetoRoot, reads the results of the pulse finder and  

writes them into a root file  

Run Parameters :  

  -rn, --Runnumber :  

    sets the runnumber [mandatory]  

  -p, --PulsePlace :  

    Path to the Output dir of the pulse finder [mandatory]  

Stage 1 Parameters :  

  -1e, --Stage1Epsilon :  

    sets allowed variation [default: 0.0015]  

  -1a, --Stage1AmplitudeTolerance :  

    sets allowed amplitude tolerance [default: 0.1]  

  -1s, --Stage1Start :  

    sets the start timebin for the optimisation [default:  

0]  

  -1e, --pStage1End :  

    sets the end timebin for the optimisation [default:  

200]

```

```

Stage 2 Parameters :
-2e, --Stage2Epsilon :
  sets allowed variation [default: 0.002]
-2a, --Stage2AmplitudeTolerance :
  sets allowed amplitude tolerance [default: 0.1]
-2s, --Stage2Start :
  sets the start timebin for the optimisation [default:
0]
-2e, --pStage2End :
  sets the end timebin for the optimisation [default: 40]

Stage 3 / Equalisation Stage Parameters :
-3s, --EqualStart :
  sets the start timebin for the optimisation [default:
0]
-3e, --EqualEnd :
  sets the end timebin for the optimisation [default:
endofpulse]

General Parameters:
-d --DebugLevel :
  Sets the debuglevel [default: 0]
-h --help:
  Shows help, exactly what you see now
-v --version:
  Show revision
example: ./writePulsesRoot.app -rn 820 -p ./teststart/

```

Correlator

```

[pcikf49:AliceTPC/AltroOptimisation/trunk] rbramm% ./correlator.
app -h
correlator, reads the results of the pulse finder and of the
makeCoefficient
Programm and builds the correlation Matrix

Run Parameters :
-rn, --Runnumber :
  sets the runnumber [mandatory]
-p, --PulsePlace :
  Path to the Output dir of the pulse finder [mandatory]

Correlation Parameters :
-w, --LevelofWidthofPulse :
  sets Level on which the width of Pulse is calculated,
  (maxADC of Pulse)*LevelofWidthofPulse [default : 0.01]
-u, --LevelofUndershootofPulse :
  sets Level on which the undershoot after the Pulse is
calculated,
  (maxADC of Pulse)*LevelofUndershootofPulse [default :
0.01]

General Parameters:
-l --listFileHeaders :
  Flag to lists the file headers
-d --DebugLevel :
  Sets the debuglevel [default: 0]
-h --help:
  Shows help, exactly what you see now
-v --version:
  Show revision
example: ./correlator.app -rn 820 -p ./teststart/

```


A:	LDC:Local Data Concentrator
ADC:Analog Digital Converter	LHC:Large Hadron Collider
ALEPH:Apparatus for LEP Physics	LHCC:LHC Committe
ALICE:A Large Ion Collider Experiment	LUT:Look up Table
ALTRO:ALICE TPC read out	LVCMOS:Low Voltage CMOS
B:	M:
BC:Board Controller	MEB:Multi Event Buffer
BCSI:Baseline Correction and Subtraction 1	MIP:Minimum Ionising Particle
BCSII:Baseline Correction and Subtraction 2	MSPS:Million Samples Per Second
C:	MWPC:Multi Wire Proportional Chamber
CASTOR:CERN Advances Storage	O:
CCL:Common Control Logic	OpenGL:Open Graphics Library
CERN:Conseil Européen pour la Recherche Nucléaire	OROC:Outer Readout Chamber
CINT:C Interpreter	P:
CMOS:Complementary Metal Oxide Semiconductor	PASA:Preamplifier/Shaper
CPU:Central Processing Unit	PCB:Printed Circuit Board
CSA:charge sensitive amplifier	PHOS:Photon Spectrometer
D:	PCI:Peripheral Component Interconnect
DAQ:Data Acquisition	PMD:Photon Multiplicity Detector
DATE:Date Acquisition Test Environment	PPR:Physics Performace Report
DIM:Distributed Information Management	ps:Postscript
DIU:Destination Interface Unit	PS:Proton Synchrotron
DCS:Detector Control System	Q:
DDL:Detector Data Link	QGP:Quark Gluon Plasma
DFU:Data Formatting Unit	R:
E:	RCU:Readout Control Unit
eps:Encapsulated Postscript	RCUI:RCU 1
F:	RCUII:RCU 2
FEC:Front End Card	RCUIII:RCU 3
FeC2:Front End Control and Configuration	RHIC:Relativistic heavy ion collider
FEE:Front End Electronics	RMS:Root Mean Square
FMD:Forwورد Multiplicity Detector	ROC:Readout Chamber
FPGA:Field Programmable Gate Array	S:
FWHM:Full Width Half Maximum	SIU:Source Interface Unit
G	SO:Shared Object
GDC:Global Data Concentrator	SPS:Super Proton Synchrotron
GIF:Graphics Interchange Format	STAR:Solenodial Traqcker At RHIC
GTL:Gunning Transceiver Logic	svg:Scalable Vector Gpahics
GUI:Graphical User Interface	T:
H:	TCF:Tail Cancellation Filter
HLT:High Level Trigger	TOF:time of flight
HMPID:high momentum particle identification	TDR:Technical Design Report
detector	TPC:time projection chamber
i:	TRD:transition radiation detector
I2C:Inter-IC	TTCRX:TT:Trigger and C:Controll and Rx: Reciever
IC:Integrated Circuit	Z:
IIR:infinite impulse response	ZDC:Zero Degree Calorimeters
IROC:Inner Readout Chamber	ZSU:Zero Suppression Unit
ISBN:International Standard Book Number	
ITS:inner tracking system	
L:	

